State of Oregon
Department of Geology and Mineral Industries
Vicki S. McConnell, State Geologist

Open-File Report O-07-14

PRELIMINARY GEOLOGIC MAP OF THE HAMAKER MOUNTAIN, WORDEN, AND LOST RIVER 7.5' QUADRANGLES, KLAMATH COUNTY, OREGON

By
Frank R. Hladky[1] and Margaret D. Jenks[1]

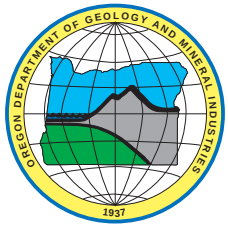

2007

[1]Oregon Department of Geology and Mineral Industries, 800 NE Oregon Street, Suite 965, Portland, Oregon 97232

NOTICE

This paper is being published as received from the author(s). No warranty, expressed or implied, is made regarding the accuracy or utility of the information described and/or contained herein, nor shall the act of distribution constitute any such warranty. This disclaimer applies both to individual use of the data and aggregate use with other data. The Oregon Department of Geology and Mineral Industries shall not be held liable for improper or incorrect use of this information.

Oregon Department of Geology and Mineral Industries Open-File Report O-07-14
Published in conformance with ORS 516.030

For copies of this publication or other information about Oregon's geology and natural resources, contact:

Nature of the Northwest Information Center
800 NE Oregon Street #5
Portland, Oregon 97232
(503) 872-2750
http://www.naturenw.org

or these DOGAMI field offices:

Baker City Field Office
1510 Campbell St.
Baker City, OR 97814-3442
Telephone (541) 523-3133
Fax (541) 523-5992

Grants Pass Field Office
5375 Monument Drive
Grants Pass, OR 97526
Telephone (541) 476-2496
Fax (541) 474-3158

For additional information:
Administrative Offices
800 NE Oregon Street, Suite 965
Portland, OR 97232
Telephone (971) 673-1555
Fax (971) 673-1562
http://www.oregongeology.com
http://egov.oregon.gov/DOGAMI/

CONTENTS

FIGURES

TABLES

1.0 INTRODUCTION

The Hamaker Mtn, Worden, and Lost River quadrangles are located in south central Oregon in the southwest part of Klamath County (Figure 1). The study area is approximately 10 km (6 mi) south of the city of Klamath Falls. The map area is part of 7.5-minute quadrangle mapping by the Oregon Department of Geology and Mineral Industries to better characterize the geologic framework in support of groundwater flow and storage studies in the Klamath Basin by other agencies. This mapping was funded in part by the U.S. Fish and Wildlife Service Hatfield Restoration Program under the auspices of the Klamath Basin Ecosystem Restoration Office.

The map area is a combination of private and public lands. The highlands are a mixture of mainly BLM and private lands. Hamaker Mountain and Chase Mountain are heavily forested and logging operations were going on during the study. Bear Valley National Wildlife Refuge, famous for its bald eagle nesting grounds, is located on the eastern flanks of Hamaker Mountain. The Klamath Hills are vegetated mainly by grasses and sagebrush. Few trees grow on Stukel Mountain except on the eastern slopes where some groves exist. The lowlands labeled “Lower Klamath National Wildlife Refuge” on the base map are, in fact, part of the Klamath Drainage District (KDD), established to drain Lower Klamath Lake. KDD is a privately owned entity and not part of the National Wildlife Refuge. Grasses and riparian vegetation occupy this area. Sagebrush encroaches on areas not under recent cultivation. Similarly, grasses and sagebrush occupy the valley of the Lost River where not under cultivation.

The principal geographic features reflect from west to east, a volcanic highland dominated by the Hamaker Mountain and Chase Mountain shield volcanoes; a structurally complex, sediment-filled, fault-bounded graben now occupied by the Klamath River; a complex horst structure at the Klamath Hills; a structurally complex, sediment-filled graben occupied by the Lost River; and the fault-bounded volcanic highlands at Stukel Mountain. Hamaker and Chase Mountains are the result of constructional volcanism of the Cascade volcanic arc. Hamaker Mountain, the larger of the two peaks, rises to nearly 6,600 feet of elevation. The nearly level surface of the Lower Klamath Lake basin, in the area of the Klamath Drainage District, results from intrabasin sedimentation. As recently as the early 20th century, Lower Klamath Lake covered this area. The Klamath Hills, which locally exceed 5,100 feet in elevation, rise as much as a 1,000 feet above their adjacent basins. The Klamath and Lost Rivers wander across the floors of these tectonic basins. The faulted volcanic highlands at Stukel Mountain rise to over 6,500 feet in elevation. The northwest-trending ridges and valleys across the map area, including the northwesterly alignment of the Klamath Hills, Stukel Mountain and the intervening valley floors, stems from extensional tectonics of the Basin and Range.

1.1 Previous Work and Methodology

Prior published mapping for the area is low-resolution reconnaissance work (1:250,000; Sherrod and Pickthorn, 1992; Peterson and McIntyre, 1970). The present mapping is the first 1:24,000 scale geologic map of the area, although there are published 1:24,000 geologic maps of the adjoining Keno (Hladky and Mertzman, 2002), Dairy (Hladky, 2003), and Merrill (Jenks and Madin, 2003) quadrangles. Pertinent to our understanding of the volcanic stratigraphy, Mertzman (2000) performed scores of K/Ar determinations for rocks of the Cascade Range in southern Oregon, a few of which are located in or near the map area and included in the table of age dates (Figure 2).

1.1.1 Mapping Methods

Geologic mapping for this project was accomplished by integrating numerous data sets. Field mapping included mapping on 7.5-minute topography sheets using observations and data collected during both foot and vehicle traverses. Field data were collected by both authors with Jenks mapping the Klamath Hills and Hladky mapping the Hamaker and Stukel Mountain areas. Stan Mertzman of Franklin

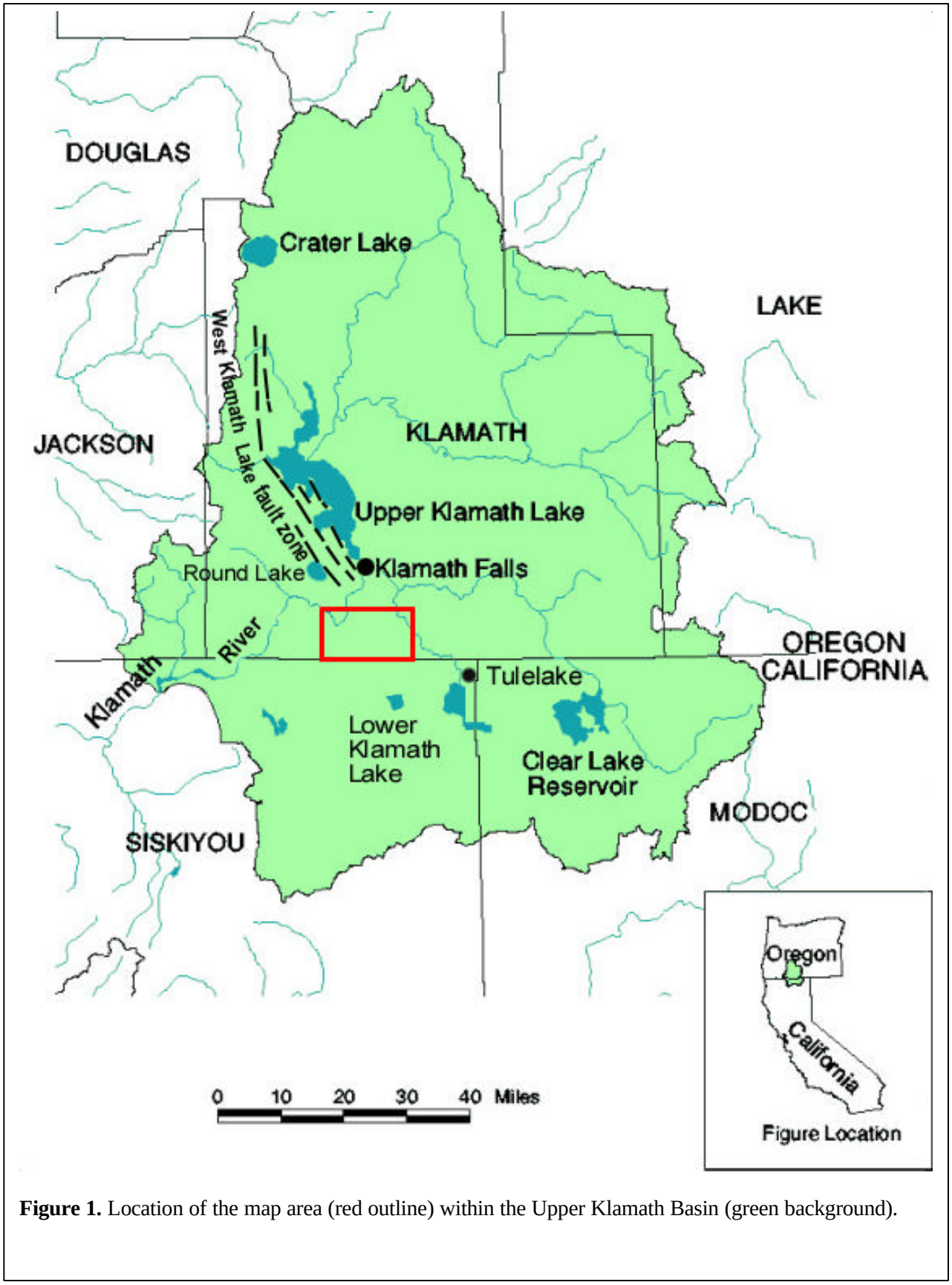

Figure 1. Location of the map area (red outline) within the Upper Klamath Basin (green background).

and Marshall College, PA, provided unpublished sketch maps of the Hamaker Mountain and Chase Mountain summit areas and some unpublished chemical analyses. Contacts were located on the ground where visible or placed based upon interpretation of topography and structure. Geologic contacts and faults were also derived from stereo black-and-white 1:31,680-scale aerial photographs by inspection or by using a Kern PG-2 stereo-plotting instrument. Poor exposure due to colluvium or soil cover on most slopes, however, often made contact delineation difficult. Hamaker Mountain and Chase Mountain are covered with dense thickets of manzanita that also impede mapping. Soil development on these mountains obscures contacts between the many basaltic andesite flows, which are similar both geochemically and petrographically.

Photographic, digital, geochemical and isotopic, and field geologic datasets were compared and reconciled both on paper and in MapInfo, a Geographic Information System (GIS) software package.

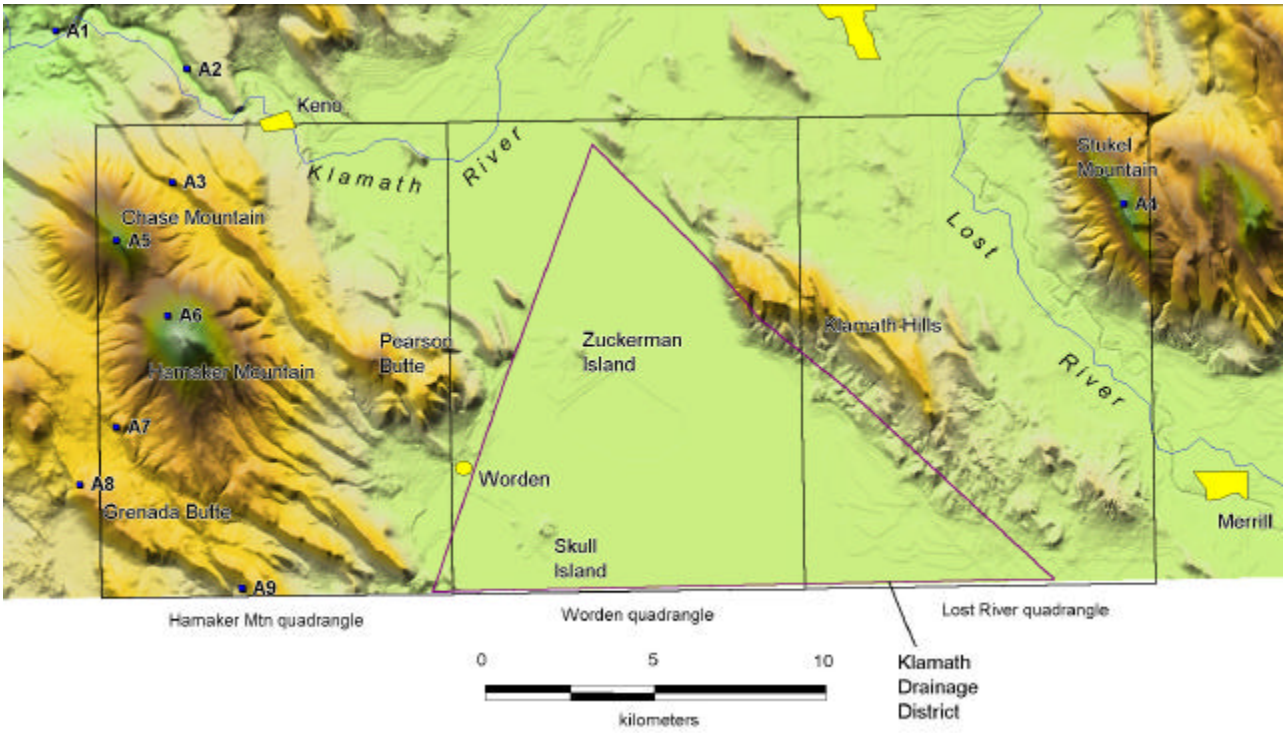

Figure 2. Map of the map area, the Klamath Drainage District, and isotopic ages. Map numbers of isotopic ages keyed to Table 2

Geologic structures were also interpreted from USGS Digital Orthophoto Quadrangles (DOQ's) and 10-m and 30-m Digital Elevation Models (DEM's). A digital version of a 1905 Klamath Basin topographic map (Figure 3) provided data on historical shorelines relevant to recent surficial deposits (U.S. Geological Survey, Reclamation Service, 1905). The geologic data collected from visual inspection of units in the field was integrated with detailed petrographic thin section descriptions, geochemical analyses (Table 1), and isotopic age data (Table 2).

Nomenclature used for volcanic rocks in the mapped area follows the International Union of Geological Sciences' chemical classification of volcanic rocks (Le Bas and Streckeisen, 1991). Volcanic samples were classified on a TAS diagram of total alkalis vs. silica (Figure 4). Classification on an AFM diagram (Figure 5), indicating relative iron enrichment (tholeiitic) or total alkali enrichment (calc-alkaline), provides indications of magma genesis and evolutionary trends for these rocks.

Volcanic flow rocks display a variety of groundmass textures observable with a petrographic microscope, and, in some cases, with a hand lens. The following list of petrographic textural terms describing the groundmass was derived from the definitions in Bates and Jackson (1987).

Texture	Description
Diktytaxitic	Groundmass feldspars protrude into jagged, irregular vesicles.
Holocrystalline	Entirely crystalline. Devoid of glass.
Hyalophitic	Glass occupies considerable space and generally either partly or wholly encloses plagioclase laths.
Hyalopilitic	Glass occupies minute interspaces between plagioclase microlites in a haphazard orientation.
Intergranular	Multiple clinopyroxene grains occupy the interstices within a network of plagioclase laths. Entirely crystalline. Devoid of glass. Grains interlock.
Intersertal	Glass occupies the minute spaces between grains.
Poikilitic	Optically continuous pyroxene completely or partially encloses laths of plagioclase.
Subophitic	Feldspar crystals are approximately the same size as pyroxene and only partially enclosed by pyroxene.
Trachytic	Alignment of feldspar microlites.

In addition, water affected lava flows strongly interact with water at the time of their eruption, but do not necessarily pillow (Jenks and Bonnichsen, 1989; Jenks, and others, 1998). The water interaction

Figure 3. Map of Lower Klamath Lake in 1905 as seen in this Bureau of Reclamation map. (U.S. Geological Survey, Reclamation Service, 1905)

causes the glassy parts of the flows, at the time of emplacement and cooling, to be altered to palagonite and other clay minerals. Unlike subaerially emplaced flows, when erosion or fault displacement exposes water affected flows to the atmospheric elements, they rapidly decompose to soils and clay. This propensity explains the general lack of good exposure for water-affected basalt flows. This interaction with water changes the percentages of the soluble elements in the analyzed samples of the water affected flows. Depending upon the degree of interaction, this water interaction leads to lower SiO_2, CaO, MgO, Na_2O, and K_2O percentages. The TiO_2, MnO, and P_2O_5 percentages appear to be unaffected, as are some of the minor elements: Zr, V, Cr, Cu, Zn, Co, and Sc.

Three geophysical surveys were conducted in the map area in 2001. A magnetic survey of the entire Klamath Drainage District (KDD) between Worden and the Klamath Hills, was done by GeoPotential Environmental and Exploration Geophysics of Gresham, Oregon. Northwest Geophysical Associates of Corvallis, Oregon performed a gravity survey of the northern part of the KDD. In addition they integrated all of the geophysical data (French and others, 2003) including three lines of seismic reflection data produced by Cooksley Geophysical of Redding, California. These studies influenced the geologic model of this study. The geophysical data were rendered in MapInfo and compared against mapped structures at the surface—the results are the interpretive subsurface lineaments shown on the map. The unpublished geophysical studies are included in Appendix A.

The log of the Thermal Power Company geothermal exploration well in sec. 35, T40S, R9E is found in Appendix B.

1.1.2 Analytical Methods

Selected volcanic rocks were analyzed for major and minor trace element chemistry by X-ray fluorescence (XRF) in the laboratory of Dr. Stanley A. Mertzman at Franklin and Marshall College, Lancaster, PA. Samples derived from lava flows were trimmed with a hammer to remove weathering rinds and obvious alteration. XRF methodology for determining rock geochemistry is described in detail in Appendix C.

Three new $^{40}Ar/^{39}Ar$ age determinations (Table 2) were performed on trimmed samples, free from obvious alteration, at the Nevada Isotope Geochronology Lab, University of Nevada, Las Vegas, NV. Detailed methodology of the dating process is explained in Appendix D.

Table 1. Whole-rock analyses, Hamaker Mtn, Worden, and Lost River quadrangles, Klamath County, Oregon. Map numbers keyed to the map. Samples with numerical sample numbers were obtained from Stanley A. Mertzman; sample numbers with a W, LR, MH, or HM prefix were collected by Frank R. Hladky; sample numbers with an MJ prefix were collected by Margaret D. Jenks. Major oxides reported in weight percent; trace elements in ppm. Fe2O3T determined by titration after the method of Reichen and Fahey (1962). All analyses by the laboratory of Stanley A. Mertzman, Franklin and Marshall College, Lancaster, PA. Eastings and northings are referable to 1927 North American datum, zone 10.

Map No.	Station No.	Sample No.	1/4	1/4	Sec.	Twnshp	Range	UTM N	UTM E	Unit	Lithology
71	--	W020725-1	NE	SE	11	40 S	8 E	4652000	596141	Tasi	Andesite
21	--	LR020802-4	SE	NE	9	40 S	10 E	4662375	612380	Tba	Basaltic andesite
22	--	KM-153	NW	SW	10	40 S	10 E	4661654	612922	Tba	Basaltic andesite
6	--	LR020806-4	NE	NE	5	40 S	10 E	4664231	610539	Tba	Basaltic andesite
9	--	LR020808-2	NE	SW	3	40 S	10 E	4663630	613195	Tba	Basaltic andesite
24	--	LR020805-1	SE	SW	9	40 S	10 E	4661321	611611	Tba	Basaltic andesite
8	--	LR020808-1	NE	NW	3	40 S	10 E	4664212	613155	Tba	Basaltic andesite
7	--	LR020806-5	SW	NW	3	40 S	10 E	4664039	612670	Tba	Basaltic andesite
38	--	LR020806-3	SW	NE	16	40 S	10 E	4659758	611835	Tbav	Basaltic andesite
56	--	W020725-2	SW	NW	34	40 S	8 E	4655583	593440	Tbaw	Basaltic andesite
76	--	MH020701-5	--	NE	14	41 S	7 E	4650869	586015	Tbg	Basalt
77	--	MH020702-2	NW	NW	16	48 N	1 W	4650314	583577	Tbg	Basalt
67	--	MH020702-8	NW	NW	12	41 S	7 E	4652779	586774	Tbg	Basalt
74	--	MH020701-3	SW	SE	11	41 S	7 E	4651477	585996	Tbg	Basalt
68	--	MH020701-6	NW	SW	10	41 S	7 E	4651737	583896	Tbg	Basalt
75	--	MH020701-4	--	NE	14	41 S	7 E	4650951	586116	Tbg	Basalt
59*	--	95-74	--	SW	4	41 S	7 E	4653390	582180	Tbg	Basalt
66	--	MH020723-2	NE	SE	6	41 S	8 E	4653414	589766	Tbgv	Basalt
79	--	MH020702-1	--	SW	16	41 S	8 E	4650574	591945	Tbgw	Basalt
72	--	MH020717-1	SW	SW	9	41 S	8 E	4651509	591841	Tbgw	Basalt
73	--	MH020702-6	SE	SE	13	41 S	7 E	4651422	588412	Tbgw	Basalt
4	--	MH020809-3	NE	SW	4	40 S	8 E	4663233	592105	Tbhc	Basaltic andesite
3	--	MH020809-2	NE	SW	4	40 S	8 E	4663260	591988	Tbhi	Basaltic andesite
18	--	MH020703-1	NE	SE	7	40 S	8 E	4661384	589798	Tbke	Basalt
12	--	MH020813-2	SW	SW	6	40 S	8 E	4662779	588454	Tbke	Basalt
26	--	MH020809-1	SE	NE	16	40 S	8 E	4660229	592846	Tbke	Basalt
27	--	MH020815-1	NE	SE	17	40 S	8 E	4659890	591400	Tbke	Basalt
65	--	W020815-2	SE	SW	34	40 S	8 E	4654507	593760	Tblm	Basaltic andesite
78	--	MH020702-3	NE	NW	14	48 N	1 W	4650340	586956	Tbm	Basalt
53	--	MH020703-3	NW	SE	29	40 S	8 E	4656836	591028	Tbpb	Basaltic andesite
44	--	MH020710-2	NE	NE	30	40 S	8 E	4657720	589808	Tbpb	Basaltic andesite
43	--	MH020703-2	SE	SW	21	40 S	8 E	4657803	592192	Tbpb	Basaltic andesite
10	--	LR020805-3	NE	SE	5	40 S	10 E	4663593	610621	Tbs	Basalt
23	--	LR020802-2	NE	NE	16	40 S	10 E	4661064	612395	Tbs	Basalt
25	--	LR020806-2	SW	SW	9	40 S	10 E	4661264	611200	Tbs	Basalt
39	--	LR020801-1	NE	NW	22	40 S	10 E	4659255	613224	Tbs	Basalt
42	--	W020816-2	SE	NE	22	40 S	8 E	4658570	594385	Tbwb	Basaltic andesite
34	--	MH020816-2	SE	NE	31	40 S	8 E	4658851	592779	Tbwb	Basaltic andesite
2	--	HM020530-1	NE	NE	2	40 S	7 E	4663839	586522	Tcm	Basaltic andesite

* Map no. 59 is located immediately west of the map area in the Chicken Hills quadrangle.

Table 1. (cont.)

Map No.	Station No.	Sample No.	SiO2	TiO2	Al2O3	Fe2O3	FeO	MnO	MgO	CaO	Na2O	K2O	P2O5	LOI	Total	Fe2O3T
71	--	W020725-1	60.58	0.65	17.51	1.73	3.10	0.09	3.03	6.13	4.01	1.32	0.56	1.51	100.22	5.18
21	--	LR020802-4	52.30	1.00	18.02	2.86	5.69	0.16	5.27	8.33	3.49	1.19	0.37	1.15	99.83	9.18
22	--	KM-153	52.44	1.10	18.05	2.97	5.51	0.16	5.06	8.16	3.50	1.25	0.42	1.03	99.65	9.09
6	--	LR020806-4	52.85	0.99	19.03	5.12	3.39	0.15	4.24	8.40	3.81	0.87	0.23	1.26	100.34	8.89
9	--	LR020808-2	52.91	1.13	18.45	2.72	5.78	0.16	3.79	7.92	3.92	1.10	0.30	1.12	99.30	9.14
24	--	LR020805-1	53.40	1.10	18.13	5.55	3.01	0.15	3.58	8.17	3.55	1.36	0.47	1.82	100.29	8.90
8	--	LR020808-1	54.54	1.07	18.01	3.16	5.18	0.15	3.46	7.48	4.10	1.03	0.21	1.12	99.51	8.92
7	--	LR020806-5	54.71	1.07	17.92	3.39	4.98	0.15	3.50	7.48	4.15	1.10	0.21	0.65	99.31	8.92
38	--	LR020806-3	52.32	1.03	17.82	4.97	3.59	0.16	4.64	8.27	3.33	1.12	0.42	2.50	100.17	8.96
56	--	W020725-2	53.47	0.78	18.73	3.67	3.96	0.12	5.00	7.91	3.73	0.94	0.19	1.78	100.28	8.07
76	--	MH020701-5	48.13	0.99	19.74	7.94	2.56	0.17	4.58	9.59	3.40	0.32	0.20	1.70	99.32	10.79
77	--	MH020702-2	48.51	1.22	16.89	4.64	5.39	0.18	6.88	11.47	2.73	0.44	0.28	0.90	99.53	10.63
67	--	MH020702-8	48.56	1.02	19.48	6.94	3.37	0.17	5.12	9.80	3.27	0.29	0.19	1.59	99.80	10.69
74	--	MH020701-3	49.52	0.92	18.67	5.44	4.15	0.16	5.76	9.87	3.18	0.45	0.18	1.51	99.81	10.05
68	--	MH020701-6	49.70	1.09	18.25	4.24	5.61	0.17	5.87	9.38	3.39	0.52	0.23	0.92	99.37	10.47
75	--	MH020701-4	49.77	1.03	18.40	3.75	5.99	0.17	6.30	9.29	3.34	0.58	0.25	0.71	99.58	10.41
59*	--	95-74	50.77	1.33	17.19	4.82	5.31	0.17	6.32	8.36	3.67	0.95	0.52	1.01	100.42	10.72
66	--	MH020723-2	50.36	1.15	19.05	5.39	4.45	0.17	4.44	9.28	3.39	0.62	0.24	1.61	100.15	10.34
79	--	MH020702-1	48.42	1.01	18.16	6.26	3.45	0.19	5.89	9.24	3.05	0.51	0.21	3.00	99.39	10.09
72	--	MH020717-1	48.49	0.95	18.53	7.58	2.56	0.14	5.34	9.13	3.05	0.38	0.17	3.89	100.21	10.43
73	--	MH020702-6	49.08	1.03	18.71	6.87	3.61	0.14	5.27	8.90	3.38	0.55	0.24	1.83	99.61	10.88
4	--	MH020809-3	55.28	0.95	18.60	2.85	4.69	0.13	3.61	7.21	4.28	1.21	0.31	0.72	99.84	8.06
3	--	MH020809-2	55.70	0.96	18.15	2.80	4.54	0.13	3.41	7.06	4.21	1.38	0.34	1.26	99.94	7.85
18	--	MH020703-1	45.47	1.00	16.78	4.86	4.71	0.17	9.91	9.58	2.27	0.14	0.08	5.45	100.42	10.09
12	--	MH020813-2	47.74	0.96	17.68	3.16	6.38	0.17	8.80	11.59	2.64	0.08	0.07	0.88	100.15	10.25
26	--	MH020809-1	47.86	1.14	17.26	7.45	3.51	0.18	7.06	10.49	2.56	0.22	0.19	2.37	100.29	11.35
27	--	MH020815-1	48.05	0.98	17.97	4.42	4.93	0.17	7.84	11.43	2.69	0.11	0.08	1.47	100.14	9.90
65	--	W020815-2	51.32	1.11	18.36	3.65	5.13	0.26	4.30	8.54	3.66	0.68	0.28	2.67	99.96	9.35
78	--	MH020702-3	48.81	1.04	18.48	4.26	5.69	0.17	6.91	8.78	3.37	0.55	0.27	1.05	99.38	10.58
53	--	MH020703-3	53.41	1.05	18.95	3.57	4.86	0.14	4.20	8.00	3.88	0.88	0.27	1.03	100.24	8.97
44	--	MH020710-2	54.40	0.82	19.13	3.07	4.31	0.12	4.19	7.72	3.94	1.01	0.20	1.07	99.98	7.86
43	--	MH020703-2	54.78	0.95	18.36	3.02	4.57	0.13	3.51	6.94	4.23	1.09	0.32	1.47	99.37	8.10
10	--	LR020805-3	48.69	1.23	17.71	8.00	2.09	0.16	5.59	8.77	3.19	0.70	0.54	3.43	100.10	10.32
23	--	LR020802-2	49.10	1.25	17.46	9.08	2.12	0.19	6.18	9.76	3.24	0.58	0.30	1.17	100.43	11.44
25	--	LR020806-2	49.74	1.20	17.62	6.22	3.74	0.17	6.45	8.88	3.50	0.75	0.42	1.17	99.86	10.38
39	--	LR020801-1	49.92	1.16	17.93	5.51	4.09	0.16	6.28	9.02	3.51	0.78	0.41	1.49	100.26	10.06
42	--	W020816-2	53.97	0.88	18.66	3.15	4.42	0.13	4.56	7.34	3.90	1.00	0.27	1.53	99.81	8.06
34	--	MH020816-2	54.10	0.89	19.00	3.62	3.91	0.13	4.26	7.36	3.93	1.01	0.28	1.31	99.80	7.97
2	--	HM020530-1	51.45	1.16	18.78	2.91	6.19	0.16	5.42	8.29	3.55	0.57	0.37	1.58	100.43	9.79

Table 1. (cont.)

Map No.	Station No.	Sample No.	Rb	Sr	Y	Zr	V	Ni	Cr	Nb	Ga	Cu	Zn	Co	Ba	La	Ce	U	Th	Sc	Pb
71	--	W020725-1	27.90	904	12.20	117	121	25	47	5.1	19.3	15	59	16	440	14	32	1	3.9	15	7.0
21	--	LR020802-4	13.60	663	21.40	133	200	65	111	7.1	19.3	75	79	29	576	18	37	<0.5	3.1	22	7.0
22	--	KM-153	15.40	639	23.70	151	211	62	94	7.3	19.4	52	82	28	608	24	42	0.9	1.9	26	7.0
6	--	LR020806-4	7.10	721	19.10	95	213	34	69	4.4	20.2	93	78	25	438	11	24	0.5	1.9	25	5.0
9	--	LR020808-2	10.50	648	22.60	139	213	16	38	6.8	21.4	74	79	25	730	19	41	<0.5	2.9	23	7.0
24	--	LR020805-1	15.80	629	27.40	158	211	18	54	7.6	19.8	62	83	24	630	20	40	0.5	2.3	24	6.0
8	--	LR020808-1	8.40	678	20.90	95	230	14	23	4.3	21.3	83	78	23	440	9	22	0.7	2.2	14	5.0
7	--	LR020806-5	10.90	679	22.80	96	231	14	22	4.3	20.9	143	79	24	406	10	25	<0.5	1.9	25	5.0
38	--	LR020806-3	12.80	637	22.90	144	201	76	136	7.6	19.3	58	88	29	527	20	40	0.6	1.8	26	7.0
56	--	W020725-2	6.90	1005	11.90	72	164	70	62	2.6	20.4	69	63	28	443	8	23	<0.5	1.7	16	3.0
76	--	MH020701-5	1.20	849	23.60	56	241	84	76	3.2	20.0	81	78	43	542	12	26	<0.5	<0.5	25	3.0
77	--	MH020702-2	4.90	520	25.50	90	238	123	310	5.3	18.7	93	68	41	400	9	24	<0.5	<0.5	29	3.0
67	--	MH020702-8	1.00	882	17.90	53	259	84	81	3.0	20.9	81	72	41	497	6	17	<0.5	<0.5	24	1.0
74	--	MH020701-3	3.30	848	15.10	54	244	77	68	3.0	19.7	70	72	39	351	8	19	<0.5	1	27	2.0
68	--	MH020701-6	2.60	825	19.40	67	243	70	57	3.4	20.9	79	71	36	387	10	24	<0.5	1	27	3.0
75	--	MH020701-4	4.30	778	17.30	60	234	79	68	3.4	19.7	78	72	37	368	10	20	<0.5	1.2	24	3.0
59*	--	95-74	9.70	650	27.50	120	218	84	202	8.2	18.1	42	99	33	502	17	39	1.2	0.6	25	4.9
66	--	MH020723-2	6.70	851	21.50	75	275	28	60	3.5	20.2	128	87	34	334	12	26	<0.5	2.2	30	3.0
79	--	MH020702-1	4.40	733	18.20	60	229	75	86	3.3	18.2	95	78	38	286	7	17	<0.5	0.7	29	3.0
72	--	MH020717-1	2.10	807	15.00	56	238	80	79	3.1	19.3	65	86	37	247	3	13	<0.5	1.3	29	3.0
73	--	MH020702-6	4.40	748	20.30	58	221	73	72	3.5	20.0	98	71	32	404	11	22	<0.5	<0.5	25	3.0
4	--	MH020809-3	12.10	849	16.20	98	183	20	20	5.3	21.1	91	74	24	556	14	30	0.6	1.3	18	5.0
3	--	MH020809-2	15.90	819	19.90	112	182	18	33	5.6	20.1	98	74	21	1535	18	40	<0.5	0.9	20	5.0
18	--	MH020703-1	1.70	263	20.90	64	190	168	219	2.4	15.8	83	65	48	90	3	9	<0.5	<0.5	29	3.0
12	--	MH020813-2	1.30	301	26.80	59	206	160	254	2.4	16.8	109	62	46	77	5	12	<0.5	<0.5	30	2.0
26	--	MH020809-1	4.20	354	24.60	71	225	138	181	3.4	17.0	99	76	43	175	3	13	<0.5	<0.5	32	4.0
27	--	MH020815-1	1.70	335	25.10	65	211	145	240	2.6	17.7	94	60	48	175	4	10	<0.5	0.8	30	3.0
65	--	W020815-2	2.60	954	19.30	96	195	42	42	4.1	20.2	76	72	31	339	14	29	0.5	1.6	23	3.0
78	--	MH020702-3	4.20	863	18.10	63	226	119	45	3.8	19.1	86	76	43	399	12	22	0.8	1.6	25	3.0
53	--	MH020703-3	5.80	1051	17.50	94	191	29	51	3.7	21.5	69	72	27	367	13	30	0.8	1.2	22	4.0
44	--	MH020710-2	7.30	991	16.00	76	171	37	36	2.8	20.9	100	66	26	844	13	27	<0.5	1.7	19	3.0
43	--	MH020703-2	9.60	896	22.00	95	170	23	21	5.0	21.1	122	76	23	553	22	37	0.7	2.2	17	4.0
10	--	LR020805-3	6.80	633	24.00	134	202	97	129	7.6	18.6	75	90	35	478	15	33	<0.5	1.1	27	5.0
23	--	LR020802-2	5.10	528	25.00	91	266	87	121	4.9	19.5	104	89	40	320	8	21	<0.5	<0.5	33	4.0
25	--	LR020806-2	7.20	650	22.90	112	225	112	139	6.5	19.0	88	88	38	429	13	27	0.7	1.7	27	4.0
39	--	LR020801-1	7.00	666	21.60	106	203	89	106	5.9	19.8	65	75	34	444	13	29	0.5	0.7	23	4.0
42	--	W020816-2	7.70	895	18.40	93	164	49	43	4.1	20.6	110	66	25	402	10	27	<0.5	1	18	3.0
34	--	MH020816-2	9.30	891	17.00	95	167	50	45	3.9	20.6	102	70	25	575	14	28	<0.5	0.7	19	3.0
2	--	HM020530-1	5.00	658	22.50	129	207	66	119	6.8	21.0	63	81	30	576	18	37	0.6	1.8	25	6.0

Table 1. (cont.)

Map No.	Station No.	Sample No.	1/4	1/4	Sec.	Twnshp	Range	UTM N	UTM E	Unit	Lithology
16	--	HM020530-4	NE	SE	9	40 S	7 E	4661424	583307	Tcm	Basaltic andesite
31	--	MH020710-4	SE	SE	16	40 S	7 E	4659530	583350	Tcm	Basaltic andesite
13	--	95-8	NE	NE	11	40 S	7 E	4662380	586360	Tcm	Basaltic andesite
15	--	HM020530-2	NE	NE	10	40 S	7 E	4662289	584906	Tcm	Basaltic andesite
1	--	MH020813-1	NW	SE	4	40 S	7 E	4663168	582700	Tcm	Basaltic andesite
45	--	MH020703-4	SW	SE	19	40 S	8 E	4658065	589213	Tcm	Basaltic andesite
32	--	95-6	--	SE	15	40 S	7 E	4659620	584460	Tcm	Basaltic andesite
14	--	95-7	NE	NE	10	40 S	7 E	4662300	584920	Tcm	Basaltic andesite
17	--	MH020710-3	NE	SW	12	40 S	7 E	4661547	587315	Tcm	Basaltic andesite
28	--	95-5	NE	NE	16	40 S	7 E	4660500	583370	Tcm	Basaltic andesite
33	--	MH020710-1	NE	NE	24	40 S	7 E	4659172	588253	Tcm	Basaltic andesite
30	--	HM020530-3	NE	NE	16	40 S	7 E	4660582	583245	Tcmd	Basaltic andesite
29	--	95-4	NE	NE	16	40 S	7 E	4660560	583270	Tcmd	Basaltic andesite
20	--	LR020805-2	NW	NW	9	40 S	10 E	4662656	610995	Td	Trachydacite dike
70	--	MH020702-5	SW	NW	12	41 S	7 E	4652235	586935	Tham	Basaltic andesite
52	--	MH020711-1	SW	SW	26	40 S	7 E	4656136	585409	Tham	Basaltic andesite
64	--	MH020723-1	SE	SW	32	40 S	8 E	4654553	590528	Tham	Basaltic andesite
51	--	MH020710-6	SW	NE	28	40 S	7 E	4656843	582762	Tham	Basaltic andesite
49	--	95-3	NE	SE	22	40 S	7 E	4658370	584770	Tham	Basaltic andesite
61	--	MH020701-1	SW	NW	3	41 S	7 E	4653876	583629	Tham	Basaltic andesite
46	--	MH020725-1	NW	NE	25	40 S	7 E	4657298	587701	Tham	Basaltic andesite
69	--	MH020702-4	SW	NE	11	41 S	7 E	4652090	585995	Tham	Basaltic andesite
63	--	MH020716-1	SW	SW	36	40 S	7 E	4654624	587148	Tham	Basaltic andesite
47	--	MH020710-5	--	NW	14	41 S	7 E	4658448	585829	Tham	Basaltic andesite
48	--	95-2	SW	SW	23	40 S	7 E	4657780	585160	Tham	Basaltic andesite
62	--	MH020701-2	SW	NE	3	41 S	7 E	4653906	584500	Tham	Basaltic andesite
60	--	MH020531-4	NE	SE	4	41 S	7 E	4653532	583132	Tham	Basaltic andesite
50	--	HM020531-2	NE	SW	22	40 S	7 E	4658162	584088	Tham	Basaltic andesite
58	--	MH020531-3	SW	NE	33	40 S	7 E	4655297	583076	Thtr	Basaltic trachyandesite
57	--	MH95-39	NE	SE	33	40 S	7 E	4655080	583270	Thtr	Basaltic trachyandesite
54	MJ02-29	MJ02-04	NE	NW	36	41 S	9 E	4656328	606931	Tbak	Basaltic andesite
41	KLAM 53769	82'-87'	NW	NE	28	40 S	9 E	4657730	602401	Tbak	Basaltic andesite
37	MJ02-45	MJ02-11	NE	NW	21	40 S	9 E	4659211	601894	Tbak	Basaltic andesite
5	MJ02-88	MJ02-26	SE	NE	1	40 S	9 E	4663472	597795	Tbak	Basaltic andesite
36	MJ02-46	MJ02-12	NE	NW	21	40 S	9 E	4659123	601850	Tbas	Basaltic andesite
40	MJ02-60	MJ02-16	NW	NE	27	40 S	9 E	4657616	603757	Tbas	Basalt
19	KLAM 53771	19'-37'	NE	NW	17	40 S	9 E	4660926	600207	Tbas	Basaltic andesite
35	MJ02-72	MJ02-21	SE	SE	17	40 S	9 E	4659812	601005	Tbas	Basaltic trachyandesite
11	MJ02-86	MJ02-25	SW	NE	8	40 S	9 E	4662077	601151	Tbas	Basaltic andesite
55	MJ01-89	MJ02-27	SW	NE	5	41 S	10 E	4654095	610615	Tv	Basaltic andesite

Table 1. (cont.)

Map No.	Station No.	Sample No.	SiO2	TiO2	Al2O3	Fe2O3	FeO	MnO	MgO	CaO	Na2O	K2O	P2O5	LOI	Total	Fe2O3T
16	--	HM020530-4	51.83	1.15	19.39	2.82	5.73	0.16	4.26	8.23	3.81	0.82	0.36	1.71	100.27	9.19
31	--	MH020710-4	53.40	1.08	18.27	2.81	5.27	0.15	4.17	8.05	3.79	1.16	0.33	1.08	99.56	8.67
13	--	95-8	53.55	1.11	17.65	2.38	6.15	0.15	5.59	8.14	3.54	1.04	0.34	0.92	100.56	9.21
15	--	HM020530-2	53.70	1.11	18.28	2.89	5.15	0.14	4.26	8.22	3.98	1.29	0.40	0.87	100.29	8.61
1	--	MH020813-1	54.14	1.07	18.04	2.28	5.61	0.14	3.97	8.00	4.02	1.22	0.35	0.77	99.61	8.51
45	--	MH020703-4	54.36	0.98	17.78	2.66	5.28	0.15	4.76	7.64	3.67	1.45	0.43	1.08	100.24	8.53
32	--	95-6	54.55	1.10	18.17	2.46	5.34	0.14	4.16	8.27	3.85	1.34	0.34	0.72	100.44	8.39
14	--	95-7	54.58	1.11	18.06	3.11	4.74	0.13	4.25	8.24	3.92	1.30	0.37	0.69	100.50	8.38
17	--	MH020710-3	54.62	0.94	17.80	3.20	4.60	0.15	4.19	7.40	3.85	1.28	0.39	1.22	99.64	8.31
28	--	95-5	54.68	1.08	18.37	2.65	5.11	0.14	4.02	8.20	3.79	1.25	0.31	0.98	100.58	8.33
33	--	MH020710-1	55.07	0.91	18.34	2.43	5.25	0.14	4.20	7.63	3.95	1.19	0.34	0.90	100.35	8.26
30	--	HM020530-3	54.25	1.06	18.48	2.18	5.63	0.14	3.77	7.92	4.03	1.23	0.34	1.05	100.08	8.44
29	--	95-4	55.01	1.12	18.09	2.23	5.62	0.14	3.90	7.87	3.92	1.22	0.31	0.97	100.40	8.48
20	--	LR020805-2	66.43	0.45	16.67	2.25	0.71	0.09	0.79	2.58	5.70	2.72	0.15	1.02	99.56	3.04
70	--	MH020702-5	53.96	0.98	17.86	3.16	4.96	0.14	4.46	7.48	3.87	1.29	0.42	1.09	99.67	8.67
52	--	MH020711-1	54.06	0.97	17.88	2.99	4.95	0.15	4.36	7.63	3.64	1.43	0.41	1.07	99.54	8.49
64	--	MH020723-1	54.14	0.97	17.79	2.43	5.31	0.17	4.44	7.70	3.78	1.34	0.42	1.28	99.77	8.33
51	--	MH020710-6	54.20	0.98	17.73	2.50	5.33	0.15	4.46	7.60	3.73	1.45	0.42	0.90	99.45	8.42
49	--	95-3	54.21	0.96	18.65	2.61	5.21	0.14	4.46	8.02	3.72	1.01	0.33	1.15	100.47	8.40
61	--	MH020701-1	54.29	1.00	17.37	2.51	5.26	0.15	4.50	7.66	3.67	1.58	0.47	0.89	99.35	8.36
46	--	MH020725-1	54.34	0.93	18.14	2.55	5.05	0.14	4.44	7.77	3.67	1.49	0.41	1.02	99.95	8.16
69	--	MH020702-4	54.52	0.98	17.50	2.89	4.89	0.15	4.38	7.37	3.80	1.42	0.45	1.11	99.46	8.32
63	--	MH020716-1	54.56	0.98	17.56	2.23	5.56	0.14	4.45	7.54	3.72	1.54	0.46	1.00	99.74	8.41
47	--	MH020710-5	54.62	0.95	18.17	2.82	4.99	0.14	3.97	7.27	4.01	1.20	0.33	1.04	99.51	8.37
48	--	95-2	54.64	0.99	18.43	6.54	1.93	0.14	3.89	7.01	3.82	1.21	0.32	1.69	100.61	8.68
62	--	MH020701-2	54.69	0.98	17.55	3.21	4.62	0.14	4.09	7.33	3.85	1.46	0.46	0.99	99.37	8.34
60	--	MH020531-4	54.71	0.99	17.48	2.58	5.17	0.15	4.19	7.38	3.84	1.44	0.45	0.87	99.25	8.33
50	--	HM020531-2	54.72	0.94	18.29	2.55	5.15	0.14	4.17	7.60	3.85	1.26	0.38	0.99	100.04	8.27
58	--	MH020531-3	52.89	1.11	17.78	5.19	3.32	0.15	4.16	7.65	3.75	1.74	0.55	1.10	99.39	8.88
57	--	MH95-39	53.07	1.13	18.06	4.31	3.94	0.14	4.50	7.91	3.69	1.74	0.51	0.61	99.61	8.69
54	MJ02-29	MJ02-04	52.69	1.07	17.08	2.21	6.62	0.16	6.02	8.16	3.32	1.27	0.41	1.23	100.24	9.57
41	KLAM 53769	82'-87'	51.13	1.17	17.13	4.56	3.96	0.14	4.52	8.51	3.43	1.18	0.49	3.67	99.89	8.96
37	MJ02-45	MJ02-11	52.63	1.37	15.91	2.95	6.89	0.18	5.59	7.73	3.25	1.55	0.54	1.49	100.08	10.61
5	MJ02-88	MJ02-26	51.26	0.99	17.85	3.11	5.28	0.14	5.52	9.30	3.29	0.57	0.21	2.05	99.57	8.98
36	MJ02-46	MJ02-12	53.81	0.93	17.82	4.62	3.23	0.15	4.42	7.74	3.68	1.07	0.26	1.98	99.71	8.21
40	MJ02-60	MJ02-16	48.75	1.42	16.34	3.01	7.51	0.19	6.69	9.38	3.13	0.66	0.50	1.78	99.36	11.36
19	KLAM 53771	19'-37'	51.14	0.94	17.24	2.66	5.60	0.14	7.14	9.02	3.12	0.78	0.29	1.30	99.37	8.88
35	MJ02-72	MJ02-21	53.46	1.11	17.41	3.17	4.97	0.14	3.94	7.64	3.67	1.69	0.59	1.70	99.49	8.69
11	MJ02-86	MJ02-25	51.77	1.17	17.67	3.12	5.17	0.15	4.88	9.56	3.38	0.81	0.26	1.59	99.53	8.87
55	MJ01-89	MJ02-27	53.35	1.01	17.87	2.15	5.73	0.14	3.96	8.08	3.71	1.18	0.23	2.28	99.69	8.52

Table 1. (cont.)

Map No.	Station No.	Sample No.	Rb	Sr	Y	Zr	V	Ni	Cr	Nb	Ga	Cu	Zn	Co	Ba	La	Ce	U	Th	Sc	Pb
16	--	HM020530-4	5.80	788	27.60	154	210	22	61	7.3	22.0	78	81	24	802	30	53	0.7	2.6	25	7.0
31	--	MH020710-4	14.70	766	22.40	146	193	22	53	7.1	21.2	65	75	24	701	22	44	0.8	1.4	23	7.0
13	--	95-8	12.50	628	20.00	117	198	79	146	7.6	19.7	69	84	27	441	17	46	0.7	1.4	24	8.9
15	--	HM020530-2	15.90	932	24.80	145	181	32	65	7.5	20.8	72	73	21	733	26	48	0.5	2.1	22	6.0
1	--	MH020813-1	17.20	798	24.50	148	191	21	49	7.1	21.4	114	75	22	642	21	42	1	2.6	22	6.0
45	--	MH020703-4	17.30	812	24.10	156	174	57	64	8.0	19.4	65	82	28	848	23	49	<0.5	1.9	21	6.0
32	--	95-6	16.90	850	22.50	152	194	24	42	7.6	21.4	80	79	21	581	22	46	1	3.3	23	8.8
14	--	95-7	16.80	934	23.00	145	203	36	58	8.1	21.1	67	80	18	638	23	49	1.3	2.9	22	6.9
17	--	MH020710-3	17.40	749	26.10	152	166	41	42	7.7	19.8	70	74	25	781	25	48	0.8	2.2	19	8.0
28	--	95-5	16.50	762	22.80	152	219	22	43	7.5	21.2	85	82	20	549	22	45	0.7	2.1	23	9.0
33	--	MH020710-1	17.90	718	22.30	140	178	34	26	7.0	20.3	80	77	24	644	19	42	1.2	1.5	22	6.0
30	--	HM020530-3	18.20	748	22.10	144	180	16	56	6.7	21.1	86	64	20	686	24	48	0.5	2.5	20	7.0
29	--	95-4	18.60	742	22.10	144	188	18	40	7.3	21.7	91	75	18	576	19	37	1.3	1.9	23	9.8
20	--	LR020805-2	30.40	440	23.40	189	32	3	2	7.5	19.8	<2	68	2	785	20	41	<0.5	3	6	8.0
70	--	MH020702-5	16.90	800	27.30	150	170	52	47	7.9	20.0	47	77	25	743	26	47	<0.5	2.4	20	6.0
52	--	MH020711-1	17.50	782	24.10	152	184	43	46	8.1	20.0	69	82	26	760	22	49	1.4	2.6	20	7.0
64	--	MH020723-1	15.90	806	22.70	152	174	57	49	7.5	20.0	88	77	27	739	23	45	0.7	0.9	20	6.0
51	--	MH020710-6	17.80	812	25.60	157	168	49	54	8.2	20.2	73	76	25	789	26	49	0.6	2.4	22	7.0
49	--	95-3	10.70	776	21.50	148	172	34	37	7.7	21.3	76	79	22	628	20	50	1.4	2.8	21	9.5
61	--	MH020701-1	18.10	970	23.20	160	177	52	60	7.9	20.2	77	79	27	959	23	50	<0.5	2.5	22	7.0
46	--	MH020725-1	17.60	796	21.70	147	173	46	56	7.7	19.1	80	79	25	738	20	46	0.6	2.3	22	7.0
69	--	MH020702-4	18.20	850	23.90	161	174	48	57	8.5	19.9	81	77	23	878	29	58	0.6	2.1	20	6.0
63	--	MH020716-1	18.70	855	23.50	162	166	45	57	8.6	20.1	66	78	25	936	24	54	0.5	1.7	19	7.0
47	--	MH020710-5	17.30	703	22.50	140	174	26	24	7.1	21.3	95	73	23	728	20	40	<0.5	1.4	21	6.0
48	--	95-2	17.80	682	19.20	130	203	36	33	7.0	21.8	57	79	22	630	18	44	1.2	1.6	19	8.7
62	--	MH020701-2	21.90	838	24.90	162	170	43	53	8.8	20.0	75	78	25	874	30	55	0.9	3.7	21	7.0
60	--	MH020531-4	19.40	844	29.30	161	165	40	47	8.6	20.2	71	78	23	875	35	61	<0.5	2.6	19	7.0
50	--	HM020531-2	16.60	754	22.40	155	174	37	45	7.7	20.0	79	78	25	762	24	49	1	2.2	21	7.0
58	--	MH020531-3	16.50	1239	23.40	171	189	65	51	7.9	20.2	73	88	28	1186	27	56	1	2.7	20	7.0
57	--	MH95-39	16.70	1284	22.80	180	198	66	59	6.4	20.5	79	86	23	1013	25	64	2.1	3	22	9.8
54	MJ02-29	MJ02-04	15.50	632	23.50	142	191	72	120	7.3	19.8	58	79	30	555	16	37	<0.5	3	23	8.0
41	KLAM 53769	82'-87'	13.40	619	25.10	144	217	71	130	7.5	20.5	64	82	27	603	18	41	0.6	1.6	25	8.0
37	MJ02-45	MJ02-11	15.10	589	24.60	157	238	74	143	7.7	19.6	82	93	31	553	21	47	0.7	0.8	27	8.0
5	MJ02-88	MJ02-26	6.00	742	17.40	72	221	65	113	4.1	19.3	88	73	30	335	7	17	0.7	2	25	5.0
36	MJ02-46	MJ02-12	7.80	1117	14.70	78	189	68	73	2.9	20.8	64	68	26	343	8	21	<0.5	1.3	21	4.0
40	MJ02-60	MJ02-16	6.00	544	27.60	106	284	102	130	5.8	19.8	105	100	42	332	12	26	<0.5	<0.5	31	5.0
19	KLAM 53771	19'-37'	9.20	697	17.80	81	220	111	189	4.9	19.1	87	78	32	385	8	20	<0.5	1	26	5.0
35	MJ02-72	MJ02-21	17.90	739	24.40	171	178	30	62	9.4	20.1	75	81	24	787	28	62	0.6	2.7	22	9.0
11	MJ02-86	MJ02-25	7.90	685	20.90	82	258	51	55	4.1	20.1	108	85	28	361	9	21	1.1	1.2	29	4.0
55	MJ01-89	MJ02-27	13.00	724	17.90	82	227	28	70	3.8	20.8	115	81	23	354	8	20	<0.5	1	26	5.0

Table 2. Isotopic ages in and near the Hamaker Mtn, Worden, and Lost River quadrangles. Eastings and northings are referable to 1927 North American datum, zone 10. Map numbers are keyed to Figure 2.

MAP NO.	SAMPLE NO.	¼	¼	Sec	Town-ship	Range	UTM_N	UTM_E	QUADRANGLE	UNIT	LITHOLOGY	METHOD	FIRST REPORTED	AGE MA
A1	95-69	SE	NE	29	39 S	7 E	4666740	581460	Spencer Creek	Tbke	Basalt	whole rock K/Ar	Hill, 1996	2.0 ± 0.3
A5	95-4	NE	NE	16	40 S	7 E	4660560	583260	Hamaker Mtn	Tcmd	Basaltic andesite	whole rock K/Ar	Hill, 1996	2.51 ± 0.07
A2	95-66	NW	NW	35	39 S	7 E	4665610	585340	Keno	Thtr	Basaltic trachyandesite	whole rock K/Ar	Hill, 1996	2.72 ± 0.19
A7	MH95-39	NE	SE	33	40 S	7 E	4655080	583260	Hamaker Mtn	Thtr	Basaltic trachyandesite	whole rock K/Ar	Mertzman, 2000	2.88 ± 0.17
A6	95-3	NE	SE	22	40 S	7 E	4658360	584770	Hamaker Mtn	Tham	Basaltic andesite	whole rock K/Ar	Mertzman, 2000	2.96 ± 0.24
A4	KM-153	NW	SW	10	40 S	10 E	4661654	612922	Lost River	Tba	Basaltic andesite	whole rock 40Ar/39Ar	this study	4.25 ± 0.04
A3	HM020530-2	NE	NE	10	40 S	7 E	4662289	584906	Hamaker Mtn	Tcm	Basaltic andesite	whole rock 40Ar/39Ar	this study	<4.72
A9	MH020702-3	NE	NW	14	48 N	1 W	4650340	586956	Hamaker Mtn	Tbm	Basalt	whole rock 40Ar/39Ar	this study	<5.89
A8	95-74	--	SW	4	41 S	7 E	4653390	582180	Chicken Hills	Tbg	Basalt	whole rock K/Ar	Mertzman, 2000	6.15 ± 0.17

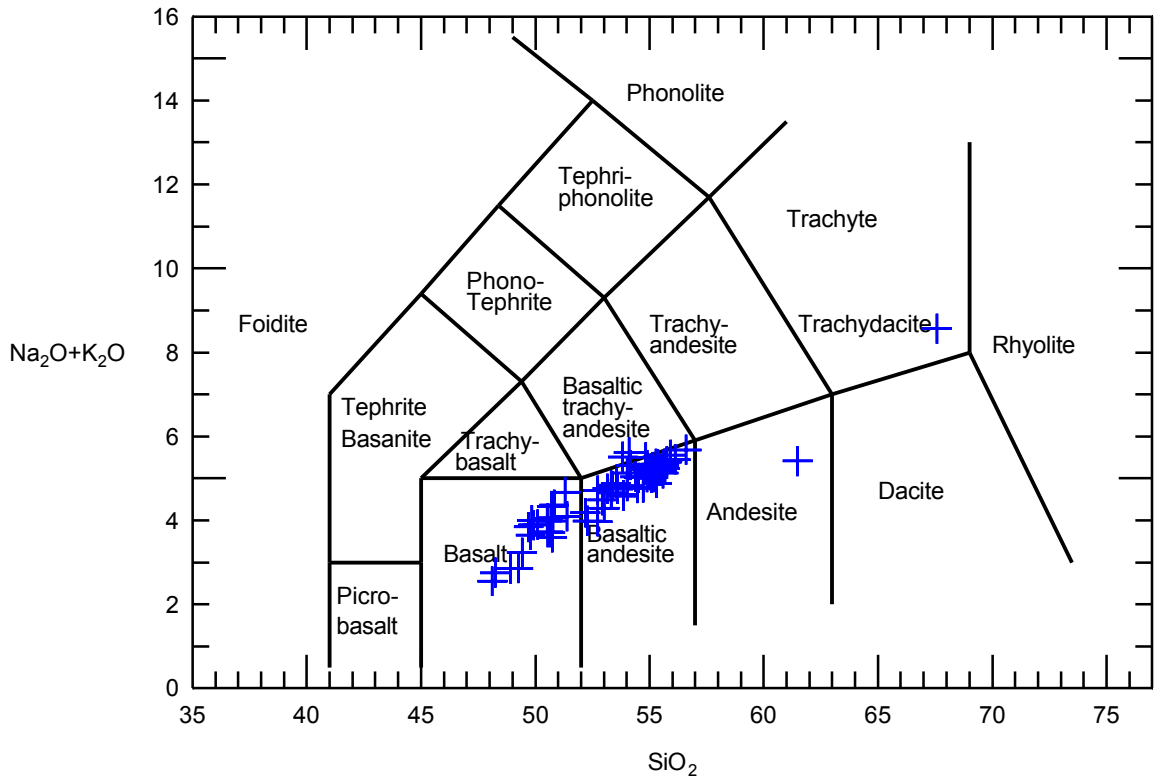

Figure 4. Le Bas and Streckeisen (1991) TAS (total alkalis vs. silica) classification for rocks in Table 1. Data have been normalized and recalculated anhydrous. Volcanic rocks in the map area range from basalt to trachydacite in composition, being predominantly basalt and basaltic andesite.

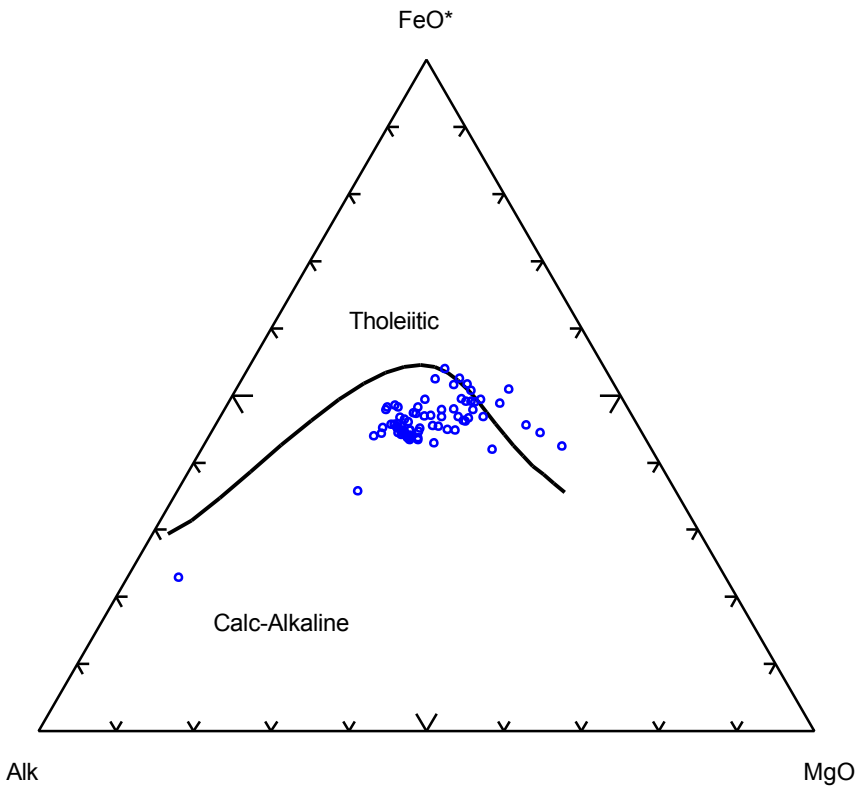

Figure 5. Irvine and Baragar (1971) AFM (total alkalis vs. silica) classification for all rocks in Table 1. Data have been normalized and recalculated anhydrous. Volcanic rocks in the map area are predominantly calc-alkaline in character.

* Fe normalized as FeO

2.0 EXPLANATION OF MAP UNITS

2.1 Surficial Deposits

Qmf **Fill (Modern)**—Unconsolidated and unsorted boulders, gravels, sands, silts, and soil that have been moved to create the dams of the small reservoirs located throughout the mapped area. Thickness is variable, depending upon the height of the dam.

Qhl **Lake deposits (Holocene)**—Unconsolidated and poorly sorted light-tan to dark-brown sand, silt, and clay, presently being deposited within the lake margins of three types of lakes. Layers of light-colored silty and sandy ash are typically interleaved with dark-brown sandy and silty loam. Includes modern deposits in man-made reservoirs. Deposits show no discernable structural deformation and conceal faults. The numerous canals and trenches that criss-cross the area and can be several meters deep, such as those in the Klamath Drainage District (KDD), might penetrate lithologically indistinguishable Pleistocene deposits, which are not mapped separately. The first type of lake includes small reservoirs located throughout the mapped area. The reservoirs catch and store irrigation and stock water, and thus are essentially dry in the Fall. In some of the lakes, cobble- to boulder-sized rocks of the nearby or underlying volcanic units lie within or on top of the fine-grained lacustrine sediments. The second type include lacustrine deposits within the area that used to be covered by the Lower Klamath Lake to the west of the Klamath Hills. Remnants of that lake include White Lake at the south end of the Klamath Hills, Lake Miller, and the lakes and marshes of the Lower Klamath National Wildlife Refuge. These lakes are principally located to the south of the mapped area in California, with only small areas reaching into the southern part of the area. The third type includes small lakes to the north and northeast of the Klamath Hills. Some of these lakes are now integrated within the irrigation system and thus have water in them year-round. However, they were originally seasonal lakes that formed in the small fault-bounded grabens within the valley floor. Spring Lake is the largest of these lakes and is located in secs. 10 and 15, T40S, R9E. Thicknesses in the small seasonal and man-made lakes and reservoirs are variable, but generally thin, due to their short histories and/or small areas. Detailed drill-core, tephrochronologic studies of some lacustrine sediments in the region indicates nearly continuous sedimentation from 3-Ma to the present (Rieck and others, 1992), without a distinct boundary between Quaternary and Tertiary sediments (Rieck and others, 1992; Adam and others, 1995). For lack of datable and mappable horizons, thicknesses of the Quaternary lacustrine sediments of the Lower Klamath Lake valley are unknown.

Qal **Alluvium (Holocene)**—Unconsolidated fluvial sediments, including clay, silt, sand, and gravel. The unit is present in the channels and meander belts of the Lost River and Klamath River. These sediments are presently being both eroded and redeposited by river flows. Due to the diversion of the main flow of the Lost River, to the north of the mapped area, for irrigation purposes, it no longer carries the same amounts of water flows and sediments that it carried in its previous, undammed state. In some areas the rivers have also been channelized to prevent flooding of adjacent farmland.

Qaf **Alluvial fan deposits (Holocene)**—Unconsolidated angular to subrounded gravel, mud, clay and soil deposited at the mouths of steep upland draws. The materials in this unit are the result of intermittent fluvial processes, primarily during thunderstorm and spring runoff flood events. The largest fans are located on the west side of the Klamath Hills and on the west flanks of Stukel Mountain. At the latter area, the fans coalesce to form a small bajada. The most significant of the fans in the Klamath Hills is in sec. 28, T40S, R9E, and is the result of the erosion of the Captain Jack draw into the pyroclastic volcanic materials on the south end of the tallest of the Klamath Hills. The smaller fans on the north side of the Klamath Hills are the result of intermittent flows from the much smaller draws incised into the fault scarp face south of Spring Lake.

Qrt **Talus deposits (Holocene)—**Unconsolidated angular boulders and blocks of volcanic rock deposited by slope processes at the foot of steep fault escarpments and other slopes. These talus deposits are unvegetated and typically have extensive networks of voids between the clasts. Mapped on the flanks of Pearson Butte in the western part of the study area and on the flanks of Stukel Mountain in the east.

Qc **Colluvium (Holocene and Pleistocene)—**Unconsolidated deposits of heterogeneous rock fragments and soil deposited by rainwash, sheetwash, or slow continuous downhill creep that obscure underlying rocks on the lower slopes of fault scarps and other steep slopes. Generally, voids between rock fragments are filled with soil, rock fragments, and vegetative matter. May include small, unmapped areas of talus.

Qs **Valley floor sediments (Holocene and Pleistocene)—**Unconsolidated, primarily fine-grained fluvial and lacustrine sediments. This unit covers the Tule Lake valley floor to the south and east from the upper historic limit of Tule Lake to the edges of the fault-bounded hills (Jenks and Madin, 2003). It is mainly a sandy silt and well logs show that it can be up to 8 m (25 ft) thick. Near fault escarpments the unit can contain a significant percentage of angular volcanic boulders and gravel. Locally, it may include aeolian sands.

Qes **Aeolian sands (Holocene and Pleistocene)—**Medium brown, subangular to well-rounded, unconsolidated lithic sand deposits. These deposits are adjacent to the present and pre-drainage shorelines of Lower Klamath Lake. The sands are lacustrine beach deposits from higher water levels of the lake. Some of the deposits, like those in the area near Midland in sec. 1, T40S, R8E, have been significantly altered and moved from their originally lake-margin positions by wind action. In this area the sand has been quarried for use by local landowners.

Qls **Landslide deposits (Holocene or Pleistocene)**—Slightly consolidated chaotic mixtures of angular rock and soil, resulting from debris flow and slump failures, or as in the case of the slide on Stukel Mountain in sec. 9, T40S, R10E, a mostly coherent glide-block of rock material originating from upslope. The mechanism for the initiation of the failures could be the result of seismic events or a wetter climate during Pleistocene glaciation. Some slides may originate where relatively weak sedimentary interbeds underlie thick lava flow sequences on steep slopes such as on the west side of Stukel Mountain. The thickness of the debris from each slide is highly variable, depending upon the particular spot within the slide deposit. The toes of each slide contain the thickest deposits.

2.2 Quaternary and Tertiary sedimentary units

QTg **Conglomerate (Pliocene-Pleistocene?)—**Pebble to boulder gravel with a sandy matrix, weakly consolidated. Clasts are predominantly basalt and basaltic andesite lavas with a lithic and feldspathic sand matrix. Boulders are up to 1 m, sub-rounded to well rounded, some interbeds of tuffaceous feldspathic sand. Interpreted as beach deposits from a Pliocene or Pleistocene high stand of a basin filling lake. In sections 22 and 23 T40S, R10E, QTg lies on a wave cut platform incised in underlying bedrock. The gravel fines from boulders to pebbles going from the north, adjacent to the highlands towards the south, suggesting that the deposits were formed by wave action in a lake occupying the Tulelake basin. Deposit is up to 15 m thick.

QTs **Valley floor sediments and sedimentary rocks (Quaternary and Tertiary)**—Unconsolidated, primarily fine-grained fluvial and lacustrine sediments, including tan, white, brown, and grey clay and subordinate sand. The unit is often offset by faults. The unit covers the valley floor to the north and east of the Klamath Hills and is also mapped on the west side of the Klamath Hills

where it occurs in fault-bounded contact with older sedimentary rocks. Also mapped in a small upland basin between Pearson Butte and Wild Horse Butte in secs. 21 and 28, T40S, R8E. While it is likely that most of these deposits are the result of recent stream and lacustrine deposition, at least part of it appears to be the faulted remnants of sediments deposited in earlier topographic configurations. Therefore, the age of the unit is problematic—some exposures clearly reflect depositional regimes that are much different from the present. For example, Manning Ridge, a small horst block in sec. 12, T40S, R9E, is capped with a deposit of well-rounded gravel, which has no association with the present drainage of the Lost River. Well logs for wells drilled throughout this part of the mapped area and north toward Klamath Falls are striking in their similarities (Appendix B). They generally consist of alternating layers of clay and silt, with up to 6 separate layers of black basaltic sands/cinders. The sand/cinder layers are traceable from well to well and offsets of them can be used to locate faults. Dating of tephra layers, extracted from drill core from various sedimentary basins in the region, indicates an age-progressive continuum with depth (Rieck and others, 1992; Adam and others, 1995). Core sampling has retrieved Pleistocene tephra in undeformed sediments within 7 meters of the surface at both the community of Tulelake (Rieck and others, 1992) and at Round Lake. Mazama tephra (7 ka) is within 2 meters of the surface at Tulelake, although it has not been found in another lake basin occupied by Round Lake. Basin sedimentation at Tulelake has been essentially continuous since 3 Ma, with periods of slow or sporadic accumulation occurring between 620,000 and 200,000 yr B.P. and between about 2.5 and 2.1 Ma (Rieck and others, 1992). Thickness of this unit ranges from a few meters on the tops of the small horsts near the valley margins, to 550 m (1,800 ft) or more below the valley floors (French and others, 2003).

2.3 Tertiary sedimentary and pyroclastic rocks

Tms **Sedimentary rocks (Pliocene and Miocene)**—Tan, white, brown, and grey, soft but consolidated, tuffaceous mudstone, with subordinate claystone and sandstone. Local drillers typically describe these layers as "chalk rock", clay, or "shale". The sediments are commonly massive, but locally thin-bedded, where sandstone or siltstone layers are present. Some layers contain a significant percentage of fresh, shiny black basaltic ash and cinders. These pre-Quaternary fine-grained sedimentary rocks are found throughout the mapped area, both as interbeds between the basalt and basaltic andesite lava flows and as thick, laterally extensive deposits. The more extensive deposits are on the flanks of the Klamath Hills, particularly on the western side and along the southern margin of the hills. Lack of isotopic ages of bounding lava flows makes the sediments poorly constrained as to their age. This lack of age control as well as poor exposures make it very difficult to sort out the stratigraphic position of particular exposures, and in many cases, even the dominant lithology of these sedimentary rocks. Similar sediments throughout the entire Klamath River basin have yielded fish fossils and diatoms that have been placed in the Miocene and Pliocene eras. Fish fossils from two locations in sec. 8, T40S, R9E have been submitted for identification. In addition, a piece of float in the area of a 30-m (100-ft) thickness of sediments in sec. 21, T40S, R9E, contained clam and snail fossils. Thickness of the unit varies widely throughout the mapped area, with some exposures having only a thin amount of sediments and others exposing 30 m or more of sediments. Geophysical and drill-hole studies in the region (French and others, 2003; Northwest Geophysical Associates, Inc., 2002; Rieck and others, 1992) indicate thicknesses of lacustrine units can be as much as 500-1,000 m (1,600-3,000 ft).

Tss **Silica-cemented sandstone deposits (Pliocene and Miocene)**—Silica-cemented, light tan to grey, fine to medium grained, well-rounded sand to pebble deposit. This unit is located throughout the southern and western fringes of the Klamath Hills, and appears to be associated with the principal valley-forming faults. The sandstone layers form prominent capping benches that are only eroded when the underlying fine-grained sediments are washed away. Beneath and sometimes interbedded with the silica-cemented sand layers are alternating layers of white to gray

claystone and siltstone, as well as layers of yellow-gold palagonitic basaltic tuff. The sand layer commonly contains some petrified wood, mostly in small pieces, but all very well preserved. Some of the outcrops also contain small clam and snail shells. In general the sand layers are thinly bedded, and some are cross-bedded. They often contain rounded rip-up clasts of the underlying white claystone/siltstone layers. The silica-cementation is likely the result of hydrothermal deposition. The present-day groundwater in the areas of the silica-cemented sandstone exposures is hot, running from 80° to 200° F (see Appendix E). In some of the sandstone outcrops the bedding is disturbed, suggesting active hot spring activity. The several exposed sections of this unit range from 3.5 m to 5 m in thickness, but the entire cemented and uncemented sandstone layers may be thicker, especially where the cementation is less marked

Tpt **Palagonitic basaltic tuff deposits (Pliocene and Miocene)—**Golden brown to orangish brown to black, generally fine-grained, palagonitized, pyroclastic tuff deposits. This unit is located across the map area: in the west near Worden, in the east on the lower flanks of Stukel Mountain, and throughout the southern part of the Klamath Hills, where it is best exposed and where it makes up small ridges. A major thickness is also exposed in the Captain Jack draw (sec. 21, T40S, R9E) and the ridges just to the south and east of that draw. In the southern part of the Klamath Hills, the tuff layers range from massive to finely layered. Some layered areas contain ripple marks and other massive layers have cinders as much as 15 cm in diameter. Some areas overly or are interbedded with the claystone and siltstone sediment layers of unit Tms. Many of the more massive layers weather to hoodoos, forming a very distinctive terrain. The tuff exposed in the Captain Jack draw grades in color from greenish in the lower part to golden in the upper part. The more golden, upper, massive tuff forms hoodoos. Most of the tuff exposures show some amount of "cold", angular, massive, lava flow pieces, ranging in size from 2 to 30 cm in diameter. Much of the tuff appears to be cemented with calcite, and the grain size varies from medium to fine sand. The entire section contains discontinuous small lava flows of water-affected basalt. A sample from the vent area dike of one of the pyroclastic volcanoes in the southern part of the hills, (map no. 55, Table 1), plots in the same area as the basaltic andesite of Short (unit Tbas), indicating the flows and these palagonitic tuff deposits may be equivalent in time, with some areas of the units having more interaction with water than others. The palagonitic tuff does unequivocally underlie the basaltic andesite of the Klamath Hills (unit Tbak), as well as varying thicknesses of fine-grained sediments (unit Tms). The base of the unit is not exposed, but the apparent thicknesses range from a few to hundreds of feet. However, again, faulting may be repeating the section to the point that it appears to be thicker than its actual measurement.

2.4 Tertiary volcanic and hypabyssal rocks near Hamaker Mountain

Chemistry (Table 1) and petrography indicate that the Hamaker Mountain area is dominanted by basaltic andesite lava flows that comprise Hamaker Mountain, Chase Mountain, Pearson Butte, and some of the buttes on the western lower Klamath Lake valley floor. In general, the chemistry of the basaltic andesite rocks are similar to each other and to other rocks in the southernmost Oregon quadrangles of the Klamath Basin, and in particular to the basaltic andesite rocks of the Stuckel Mountain area in the Dairy and Merrill quadrangles to the east of the Klamath Hills (Hladky, 2003; Jenks and Madin, 2003).

However, extensive basalt flows are also found in the southwest part of the mapped area, near the California border, including the basalt of Grenada Butte, a megacrystic basalt unit, and the diktytaxitic, tholeiitic basalt of Keno. The latter crops out extensively near the Klamath River. Most of the basalt lavas in the map area are calc-alkaline in character (Figure 6). The occurrence of tholeiitic basalt, particularly high-alumina olivine tholeiite (HAOT), such as the basalt of Keno, is interesting because HAOT is associated with back-arc spreading in extensional terrains, such as the Basin and Range (Hart and others, 1984). Tholeiitic lavas are rare in the Cascade arc in southern Oregon, where calc-alkaline lavas tend to dominate the constructional volcanism (Mertzman, 1996).

Tholeiitic basalt lava flows in the map area tend to be distinctly diktytaxitic while calc-alkaline flows tend to be glassy to intergranular. Of the older lavas, the basalt of Grenada Butte (unit Tbg) is generally calc-alkaline, even though its texture is usually dikytaxitic, an unusual texture for a calc-alkaline basalt unit. Related facies of the basalt of Grenada Butte--the vent facies lavas (Tbgv) and water-affected lavas (Tbgw)--despite their alteration, are chemically similar to the unaltered flow facies. The

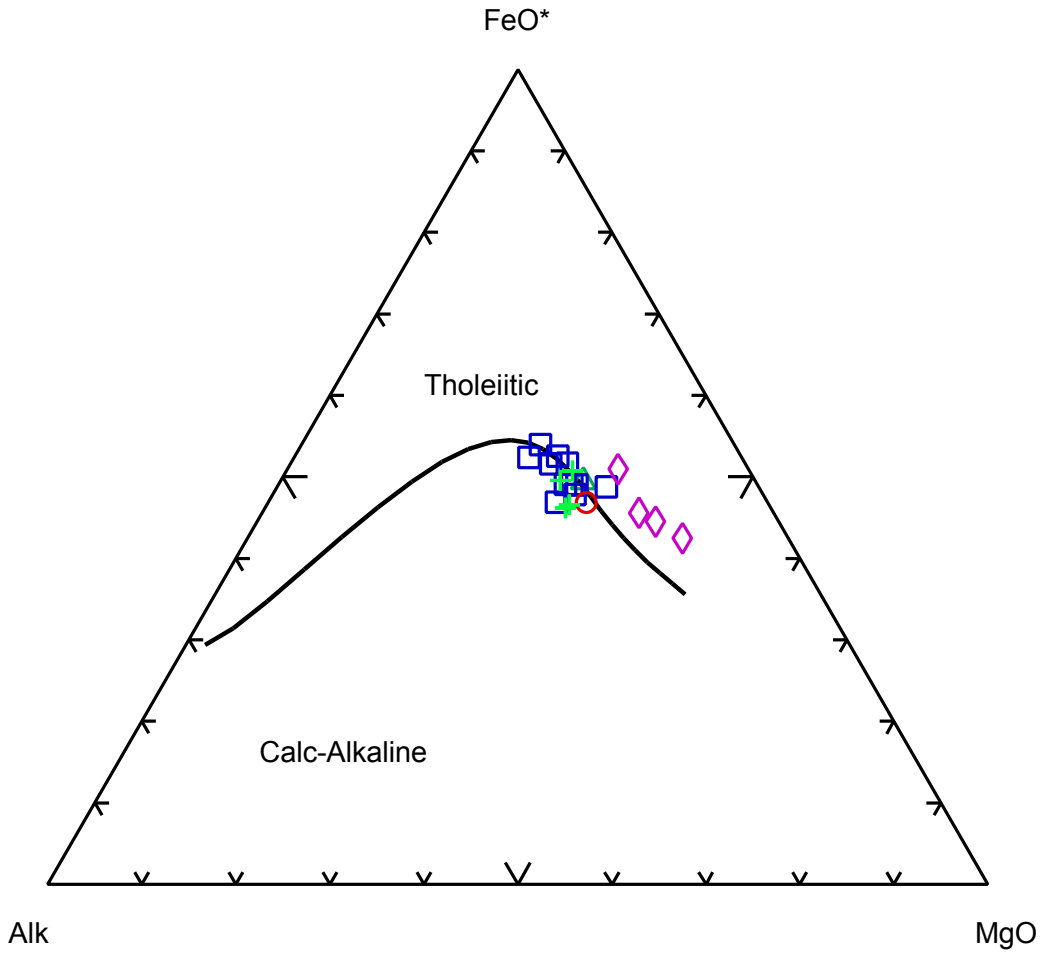

Figure 6. Irvine and Baragar (1971) AFM (total alkalis vs. silica) classification for some of the volcanic rocks of the Hamaker Mtn area. Data have been normalized and recalculated anhydrous. Volcanic rocks in the map area are predominantly calc-alkaline in character. The tholeiitic basalt of Keno is a notable exception. Rocks of the basalt of Grenada Butte are mostly calc-alkaline, although a few samples lie within the tholeiite field.

Triangle	Basalt of Short
Squares	Basalt of Grenada Butte
Diamonds	Basalt of Keno
Circle	Megacrystic basalt
Crosses	Basalt of Stukel Mountain

basalt flows at Stukel Mountain are also calc-alkaline (Figure 6). The only andesite lava flows in the mapped area are limited to Skull Island.

In all areas, where lava flows are in close contact with sediments, they may be water affected. Because most of the sediment exposures are located near the valley floors, this area is also the location of the water-affected lava flows. Flows at Horsehead Island on the valley floor, however, are not water-affected, attesting to local dry vent conditions.

Tbhc **Basaltic andesite cinders and lava of Horsehead Island (Pliocene)—**Mostly dark-gray, layered cinders with thin (< few meters) interleaved lava flows. Flows consist of mottled tan- and gray-weathering, slightly reddish-brown, medium-gray, fine-grained, basaltic andesite, with >55 weight percent SiO_2 and >18 weight percent Al_2O_3 (Table 1, map no. 4). Microvesicles are a common component (up to 7 percent) of cinders, which are glassy and aphanitic. In thin section, flows contain 1-2 percent iddingsitized crystals olivine <0.5 mm; plagioclase phenocrysts 0.5-1.5 mm, 5 percent; very fine plagioclase <0.5 mm comprise 20-30 percent; black glass is about 60 percent. Hyalophitic texture. The deposits at Horsehead Island (sec. 4, T40S, R8E) dip radially away the vent area. The unit is surrounded by Holocene lacustrine deposits, which lap up to the sides of the small butte. The cinder cone likely erupted through older valley fill deposits, now covered by Holocene lacustrine deposits. No palagonitization is evident, indicating dry conditions at the vent. Because of the unit's isolated position relative to other volcanic units and the lack of age data, its stratigraphic position is uncertain. Deposits are at least 60 m (200 ft) thick.

Tbhi **Basaltic andesite of Horsehead Island (Pliocene)—**Mottled, tan- and gray-weathering, slightly reddish-brown, medium-gray, fine-grained to slightly porphyritic, basaltic andesite lava flows. Basaltic andesite in composition with 55-56 weight percent SiO_2 and ~18 weight percent Al_2O_3 (Table 1, map no. 3). Microvesicles are rare. In thin section the flows contain slightly iddingsitized olivine up to 1 mm, though generally <0.5 mm, 1-2 percent; orthopyroxene <0.5 mm, <1 percent; glomerocrysts of many small phenocrysts of plagioclase, 5-10 percent; plagioclase <0.5 mm, 50-60 percent; dark-gray glass, about 30 percent; and a trace of very fine magnetite. Groundmass texture ranges from intergranular to hyalophitic. Located at Horsehead Island (sec. 4, T40S, R8E), these flows emanated from the flanks of that cinder cone. Post-eruption faulting is indicated by the abrupt, linear high-angle contact of the flows with the cinder deposits. Thickness exceeds 30 m (100 ft).

Tasi **Andesite of Skull Island (Pliocene)—**Orangish-tan and gray weathering, medium dark-gray, fine-grained to glassy, andesite flows at Skull Island. Andesitic in composition with ~60 weight percent SiO_2 (Table 1, map no. 71), which makes it different from any other lava flows in the map area. Generally massive to blocky with joint spacing up to 1 m, includes local randomly incorporated reddish-brown agglutinous lava, spatter, scoria, and breadcrust bombs up to 30 cm long. In thin section flows display rare, slender hornblende crystals up to 1 mm long; rare microphenocrysts of clinopyroxene <0.5 mm; 10-15 percent slender feldspar microlites, usually <0.2 mm long; 5-7 percent microvesicles <0.5 mm; set in a matrix of dark-gray glass with traces of magnetite, comprising 85-90 percent. Distinctive felty, hyalopilitic texture. Skull Island (sec. 11, T41S, R8E) is an erosion-resistant volcanic butte surrounded by Quaternary lacustrine and aeolian sediments. At the southeast corner of the island, lava flows overlie exposed white consolidated ashy mudstone (unit Tms) containing embedded blocks up to 30 cm of andesite. Since similar lacustrine sediments cover a wide range of ages and there are no capping units of known age, the age of the andesite of Skull Island remains enigmatic. Aeolian sands abut the southwest edge of the island and have been excavated for mass graves filled with the carcasses and bones of dead cattle. Maximum thickness unknown, but as much as 30 m (100 ft).

Tbke **Basalt of Keno (Pliocene)—**Mottled, brown- and gray-weathering, medium-gray to medium-light-gray with a slight reddish-brown tint, fine-grained, strongly diktytaxitic basalt. Usually massive. Tholeiitic basalt in composition, the unit is distinguished chemically by its low SiO_2

content (45-48 weight percent) and high proportions of iron and magnesium (Table 1, map nos. 12, 18, 26, and 27). Olivine <0.5 mm, typically with iddingsitized rims, 5-10 percent; 50-60 percent pyroxene 0.5-2 mm with nearly equal shares of clinopyroxene (somewhat more abundant) and orthopyroxene. Pyroxene poikilitically encloses and/or partially encloses laths of plagioclase up to 1 mm, but generally <0.5 mm; plagioclase comprises 30-35 percent. While strongly diktytaxitic in hand sample, in thin section poikilitic texture is characteristic of the basalt of Keno. Contains a trace to one percent of very fine magnetite. Randomly and sporadically water-affected over distances of tens of meters, the basalt turns mottled dark-gray- and brown-weathering, olive-black, and fine-grained and palagonitic, often losing its diktytaxitic texture in hand sample but retaining the poikilitic, albeit somewhat altered, relationships in thin section (Table 1, map no. 18). Whole-rock K-Ar age of 2.0±0.3 Ma (Table 2). Thickness exceeds 100 m (300 ft).

Tcm **Basaltic andesite of Chase Mtn (Pliocene)—**Orangish-tan weathering, medium-light to medium-dark gray, fine-grained to slightly porphyritic, massive to tabular, dense, basaltic andesite. Weathers to decimeter to meter-scale subangular to rounded blocks and boulders. Chemically basaltic andesite in composition with ~52-55 weight percent SiO_2 and >17 weight percent Al_2O_3 (Table 1, map nos. 1, 2, 13, 14, 15, 16, 17, 28, 31, 32, 33, and 45). In thin section, slightly iddingsitized olivine <0.5 mm comprises 1-2 percent; orthopyroxene <0.5 mm comprises up to 1 percent; plagioclase phenocrysts 0.5-1 mm comprise 10 percent, plagioclase microlites and microphenocrysts <0.5 mm comprise 60-65 percent, dark-gray glass comprises 25-30 percent; extremely small magnetite is <1 percent. Intersertal texture in thin section. The original age assigned to these flows is from a K-Ar age of 2.51 ± 0.07 Ma taken from the summit area of Chase Mountain (Mertzman, 2000; Hladky and Mertzman, 2002). Mapping from this study indicates that the summit area sampled is dike rock (unit Tcmd), probably related to summit eruptions—a youngest age limit. A new $^{40}Ar/^{39}Ar$ age determination from a flank flow (Table 2, map no. A3) was somewhat inconclusive: ranging from 2.08 Ma to 4.7 Ma. The sample had a generally U-shaped age spectrum with an initial step age of 117 Ma, followed by decreasing ages, then rising and somewhat discordant ages with the final steps. There was no plateau defined but a total gas age is 4.72 ± 0.05 Ma. The sample did not have an isochron. There are two possible interpretations: (1) the total gas age of 4.7 is a maximum age or (2) the youngest age on the age spectrum (2.08 Ma) is a maximum age (strongly U-shaped age spectra can indicate excess argon, which yields an overestimation of age). The relationship of these flows to the age of rocks at the summit (unit Tcmd) and to the age of rocks at Hamaker Mountain, indicates that Chase Mountain was built through volcanic eruptions between 2.5-3.0 Ma. Thus, although stratigraphic relationships are somewhat ambiguous, Chase Mountain is still considered a slightly younger satellite volcano to the larger Hamaker Mountain edifice (Mertzman, 2003, personal comm.)

Tcmd **Basaltic andesite dike of Chase Mtn (Pliocene)—**Light-gray basaltic andesite dike, at the summit of Chase Mtn. Weathers to light-colored tablets that are decimeter size. Basaltic andesite in composition with 54-55 weight percent SiO_2 and >18 weight percent Al_2O_3 (Table 1, map nos. 29, and 30). Major oxides and minor elements fall within the range of variation found in basaltic andesite flows of Chase Mountain. In thin section, comprised of about 10 percent fresh olivine <0.5 mm; 3-4 percent orthopyroxene <0.5 mm; 1-2 percent clinopyroxene <0.5 mm; 80 percent interlocking plagioclase generally <0.5 mm but up to 1 mm; 5 percent magnetite <0.2 mm; and about 5 percent glass. Texture is predominantly intergranular. K-Ar age of 2.51 ± 0.07 Ma (Table 2, map no. A5). This dike probably fed some of the youngest flows, at least the youngest flows around the summit.

Tham **Basaltic andesite of Hamaker Mtn (Pliocene)—**Orangish-tan-weathering and gray-weathering, medium-gray, fine-grained, basaltic andesite. Usually massive. Weathers to decimeter to meter-scale subangular to rounded blocks and boulders. Neither petrographically or geochemically

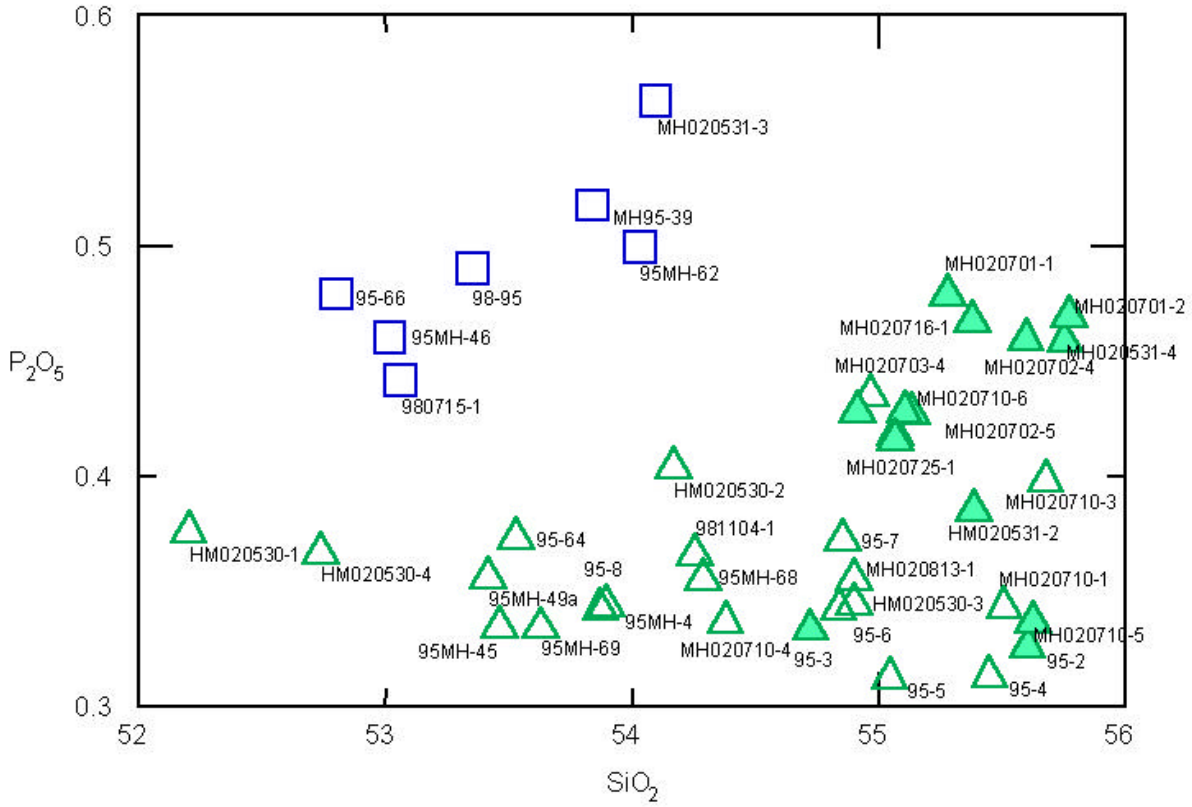

Figure 7. P_2O_5 vs. SiO_2 for basaltic andesitic lava flows at Chase Mountain and Hamaker Mountain. The basaltic andesite flows are represented by triangles (unit Tham=closed green triangles, unit Tcm=open green triangles). The basaltic andesites from the two volcanoes are not geochemically distinct, although the flows from Chase Mountain include a much broader range of silica values. Basaltic trachyandesite (unit Thtr) from Hamaker Mountain, some of the earliest lavas from the mountain, are represented by blue squares. Basaltic trachyandesite, as a lithology, is somewhat higher in K_2O and Na_2O than basaltic andesite, but the difference units tends to be gradational. This plot allows us to see how unit Thtr is geochemically distinct, tending toward higher P_2O_5 values relative to SiO_2. P_2O_5 was chosen because elevated P_2O_5 values have been associated with other alkaline rocks in the Cascade Range (Hladky, 1998). This plot includes data, normalized and calculated anhydrous, from Table 1 (this study) and from the Keno quadrangle (Hladky and Mertzman, 2002). Sample numbers, which are unique, rather than map numbers which are not, are used to identify the individual data points from the two papers.

distinguishable from basaltic andesite of Chase Mountain. Geochemically this unit is basaltic andesite in composition, with SiO_2 content consistently near 54 weight percent, a narrower range than Chase Mountain flows (Figure 7); Al_2O_3 content is >17 weight percent, and other major elements occupy similar ranges as the Chase Mountain flow although P_2O_5 is generally elevated (Figure 7, Table 1, map nos. 46, 47, 48, 49, 50, 51, 52, 60, 61, 62, 63, 64, 69, 70). Petrographically, contains microvesicles <0.5 mm, <1-5 percent. Plagioclase phenocrysts 0.5 mm-1 mm, about 3 percent; microphenocrysts of plagioclase 0.2-0.5 mm, 30-50 percent; slightly iddingsitized olivine, <0.5 mm, 3-5 percent; clinopyroxene <0.5 mm, <3 percent; trace of clinopyroxene; set in matrix of plagioclase microlites, 20-25 percent, black glass 25-30 percent, extremely fine pyroxene <10 percent and magnetite <3 percent. Texture is hyalopilitic. Hamaker Mountain and Chase Mountain comprise a composite shield volcano composed of mostly basaltic

andesite lava flows. Age data indicate that Hamaker Mountain is the main cone that erupted first. Chase Mountain is a major satellite cone that developed somewhat later. K-Ar age of 2.96 ± 0.24 Ma (Table 2, map no. A7). These flows comprise the bulk of Hamaker Mountain. Overlies basaltic trachyandesite of Hamaker Mtn, which has flows with age ranges that overlap the single date for this unit.

Thtr **Basaltic trachyandesite of Hamaker Mtn (Pliocene)—**Brownish-gray-weathering, dark-gray, fine-grained, vesicular, basaltic andesite. Geochemically a basaltic trachyandesite with 52-53 weight percent SiO_2 and >5 weight percent total alkalis (Na_2O and K_2O) (Table 1, map nos. 57 and 58). These alkaline flows also have elevated concentrations of P_2O_5 (Figure 7), a geochemical characteristic of alkaline rocks in the Cascade Range (Hladky, 1998). In thin section, the rock consists of up to ten percent vesicles, 2-3 mm; 1-2 percent iddingsitized olivine, <0.5 mm; 5-10 percent groundmass clinopyroxene, <0.2 mm; 50-60 percent plagioclase, <0.5 mm, at some locations up to 1 mm; 30-40 percent black glass. Texture is hyalophitic. K-Ar age of 2.72±0.19 Ma for geochemically similar, far-traveled flows found in the Klamath River Canyon downstream of Keno (Table 2, map no. A2). K-Ar age of 2.88 ± 0.17 Ma on south flank of Hamaker Mtn (Table 2, map no. A7). The ages for this lithology overlap that of the basaltic andesite flows of Hamaker Mountain that overlie these basal, alkaline flows. The age overlap indicates that the Hamaker Mountain edifice was built over a geologically short period of time. Thickness >200 ft (70 m).

Tbpb **Basaltic andesite of Pearson Butte (Pliocene)—**Pale-olive-gray to medium-gray, fine-grained to porphyritic, dense, olivine basaltic andesite. Weathers to rounded boulders. Breaks concoidally where unaltered. Basaltic andesitic in composition with 53-55 weight percent SiO_2 and >18 weight percent Al_2O_3 (Table 1, map nos. 43, 44, 53). In thin section, comprised of 5-15 percent olivine, occasionally iddingsitized, <0.5 mm; 5 percent pyroxene, mostly clinopyroxene but some orthopyroxene; 15 percent seriate plagioclase phenocrysts, 0.5-2 mm, 20-30 percent plagioclase, <0.5 mm; 10 percent greenish-gray glass; 2-3 percent magnetite <0.1 mm. Texture is intersertal to hyalophitic. Flows emanate from an eroded volcano in secs. 28, 29, 32, and 33, T40S, R8E. Agglutinous, vesicular and glassy zones concentrated in sec. 29 indicate the eruptive center is immediately east of the present summit of Pearson Butte. Field relationships are somewhat ambiguous because of poor contact exposure, but map relations indicate that flows from Hamaker and Chase Mountains are probably younger, being banked in against the Pearson Butte edifice. Thickness >300 m (1,000 ft).

Tbaw **Basaltic andesite of Worden (Pliocene)—**Reddish-brown-weathering where iron-stained, otherwise medium-light-gray-weathering, medium-light-gray, glomerocrystic, clinopyroxene, basaltic andesite. Tabular. Dark clinopyroxene phenocrysts lend a speckled appearance to the light-colored rock. Adjacent to and geochemically similar to the basaltic andesite of Pearson Butte, although slightly depleted in TiO_2 and doubly enriched in Ni (Table 1, map no. 56). In thin section, about 2-3 percent olivine, <0.5 mm, usually partially iddingsitized or enclosed or partially enclosed in green celadonite or chlorite; 7-10 percent clinopyroxene, <0.5 mm, often in glomerocrystic clumps up to 5 mm; trace to 1 percent magnetite, <0.2 mm; plagioclase, <1 mm, 80-85 percent; green celadonite or chlorite 2-3 percent. The rock is holocrystalline (intergranular). This texture indicates a hypabyssal intrusive rock and this unit may represent a small, magmatically-related, laccolith or dike coeval with the lava flows at Pearson Butte. Limited to sec. 34, T40S, R8E.

Tbwb **Basaltic andesite of Wild Horse Butte (Pliocene)—**Brownish-orange-weathering, fine- to medium-grained, medium-gray to medium-dark-gray, slightly porphyritic, basaltic andesite. Both agglutinous and tabular zones in outcrop. Agglutinous zones are reddish brown and usually aphanitic. Geochemically the unit is basaltic andesite, with 53-55 weight percent SiO_2 and >18 weight percent Al_2O_3 (Table 1, map nos. 34 and 42). In thin section, about 7 percent very fine

olivine, <0.5 mm, always partially iddingsitized, usually along its rims; one percent very fine orthopyroxene, <0.2 mm; 50-60 percent seriate plagioclase, <2 mm, 10 percent as phenocrysts 0.5-2 mm; 20-25 percent dark gray glass; 2-3 percent very fine magnetite <0.2 mm. Intersertal texture. Upholds fault-bounded buttes north of Worden in secs. 22, 23, 26, and 27, T40S, R8E. The Flowers Quarry in sec. 23 exposes the Wild Horse Butte Fault surface on the west side of Wild Horse Butte. There, the rock is polished to smooth, curvi-planar slickensides on the outer surface of the fault gouge. The slickensides dip 55-65 degrees. The fault gouge is 2-5 cm thick and incorporates cm-size angular clasts of basaltic andesite—perhaps colluvium. The fault tip cuts through thin colluvium in the upper part of the outcrop. The colluvium is found on both the hanging wall and the footwall. At Wild Horse Butte, the colluvium is too thin and discontinuous to map at the current scale. Stratigraphic relationships are imprecise because of lack of contacts with units of known age. The basalt of Keno is banked in against the unit, indicating a minimum age. Thickness exceeds 120 m (400 ft).

Tblm **Basaltic andesite of Lake Miller (Pliocene)—**Mottled gray- and goldish-brown-weathering, brownish-gray and dark-olive-gray, fine-grained, palagonitized basaltic andesite. Palagonitized basaltic andesite flows chemically similar to other basaltic andesites in the region, although lower in SiO_2, depleted in water-mobilized elements of K_20 and Rb, and exhibiting high loss on ignition (Table 1, map no. 65)—probably due to being water-affected. The flows are thin and locally scoriaceous. Comprised of 1-2 percent iddingsitized olivine, <0.5 mm, palagonite at many sites replaces olivine; 2-5 percent extremely fine clinopyroxene, <0.1 mm; 50-60 percent plagioclase <0.5 mm; 10-15 percent green palagonite; 10 percent dark-gray glass; 1-2 percent extremely fine magnetite; zeolite noted in hand sample. Texture is intersertal. Mapped at Worden (sec. 34, T40S, R8E and sec.3, T41S, R8E) and Zuckerman Island (sec. 25, T40S, R8E). Overlies palagonitic tuff near Worden. However, the palagonitic tuff is not a good stratigraphic marker because of its wide spatial and temporal range. Since the unit caps the Zuckerman Island horst at Zuckerman Island it is probably of a similar stratigraphic position as the basaltic andesite of Wild Horse Butte, which is exposed by the same horst at Wild Horse Butte. Thickness less than 20 m (60 ft).

Tbg **Basalt of Grenada Butte (Miocene)—**Generally gray-weathering but also brown- to tan-weathering, medium-gray, coarse-grained, slightly to moderately diktytaxitic olivine basalt. Basalt in composition with <50 weight percent SiO_2 (Table 1; map no.s 59, 67, 68, 74, 75, 76, 77). The ratio of alkaline elements (Na_2O and K_2O) to iron and magnesium indicate that these basalt rocks are calc-alkaline, although some samples are nearly tholeiitic (Figure 6). This chemistry is unusual given that diktytaxitic flows in the region are typically tholeiitic. In thin section spherical vesicles and irregular voids up to 1 mm comprise 5-10 percent; anhedral clinopyroxene generally <0.5 mm comprise 15-20 percent; 5 percent subhedral to euhedral red iddingsitzed olivine up to 2 mm; 70 percent seriate plagioclase 0.2-1 mm; 5 percent irregular-shaped magnetite <0.5 mm. Trace of glass. Texture is intergranular. Overlain by younger flows of Hamaker Mountain—the contact indicates modest relief on its upper surface. The unit is underlain variously by water-affected basalt of Grenada Butte and megacrystic basalt. Whole rock K-Ar age of 6.15 ± 0.17 Ma (Table 2, map no. A8). Thickness exceeds 240 m (800 ft)

Tbgw **Water-affected basalt of Grenada Butte (Miocene)—**Gray- to tan-weathering, dark-gray, fine-grained, sometimes pillowed basalt. Exposed surfaces weather to hard unaltered irregular basalt nodules of decimeter to meter size in a goldish-tan, clay-rich granular matrix that weathers to a dusty sand. Basalt in composition with 48-49 weight percent SiO_2 (Table 1; map no.s 72, 73, and 79). Major oxide and trace element abundances correlate well with the basalt of Grenada Butte, except for Ba which is depleted. In thin section, the less altered nodules are comprised of 5 percent red iddingsitized olivine 0.2-2 mm, mostly <0.5 mm; 5-10 percent plagioclase phenocrysts 0.5-2 mm; trace of altered orthopyroxene <0.5 mm; 20-30 percent plagioclase microlites <0.3 mm long; 40-50 dark-gray magnetite-bearing glass; about 5 percent green celadonite or gold palagonite. The texture is hyalopilitic to intersertal. Exposed in the vicinity of

Worden and Miller Lake, generally grades upward into unaltered basalt of Grenada Butte, except in sec. 33, T40S, R8E and sec. 4, T41S, R8E. where it is directly overlain by flows from Hamaker Mountain. Underlain by either palagonitic tuff or lacustrine sediments. Alteration indicates water-lava interaction without fragmentation of the lava flows. Thickness up to 30 m (100 ft)

Tbgv **Basaltic vent agglutinate of Grenada Butte (Miocene)—**Reddish-orange-weathering, dark-reddish brown, porphyritic breadcrust bombs, agglutinate, and cinders. Correlates geochemically with basalt of Grenada Butte (Table 1, map no. 66). Coeval with flows of basalt of Grenada Butte and overlain by much younger basaltic andesite flows from Hamaker Mountain. In thin section, plagioclase 0.5-5 mm, 5-7 percent; iddingsitized olivine <0.5 mm, 10 percent, rarely up to 1 mm; matrix of 25-30 percent feldspar microlites (<0.1 mm) and black glass, 50 percent. Texture is hyalopilitic. The exposures in secs. 5 and 6, T41S, R8E have been quarried for road cinders. These small deposits are the only exposed vent deposits associated with the basalt of Grenada Butte in the map area. Others undoubtedly exist, but are obscured by younger flows or hidden within thick vegetation. Thickness exceeds 30 m (100 ft)

Tbgl **Basaltic lahar deposits of Grenada Butte (Miocene)—**Rounded basaltic boulders up to 0.5 m in a chaotic mudstone and granular matrix, generally clast-supported. Basalt boulders are generally penetratively altered and weathered, slightly diktytaxitic to porphyritic. Field relations indicate a spatial relationship to vent facies of the Grenada Butte volcanic rocks. Exposed only in sec. 6, T41S, R8E. Thickness 10 m (30 ft)

Tbm **Megacrystic basalt (Miocene)—**Gray-weathering, medium-dark-gray, fine-grained, massive to tabular flows of porphyritic basalt. Characterized by megacrysts and glomerocrysts of plagioclase up to 5-10 mm, often glomerocrystic with olivine. Forms blocky boulder-sized talus piles on steep slopes. Basalt in composition with <49 weight percent SiO_2 (Table 1, map no. 78). In thin section consists of about 10 percent megacrysts of plagioclase 2-10 mm; 5 percent partially iddingsitized olivine 1-4 mm; 5-10 percent olivine <0.5 mm; <5 percent clinopyroxene <0.2 mm; 3-5 percent magnetite <0.5 mm; 60 percent plagioclase <0.5 mm; <5 percent glass. Texture is intergranular. Exposed on the Oregon-California border in the southwestern part of the map area. Whole rock $^{40}Ar/^{39}Ar$ maximum age of 5.9 Ma (Table 2, map no. A9). Overlain by the basalt of Grenada Butte. Its age, which has a low-level of precision, and field relationships suggest it was erupted slightly before the basalt of Grenada Butte. Thickness up to 100 m (300 ft)

2.5 Tertiary volcanic rocks of the Klamath Hills

The Klamath Hills contains three different types of hydroclastic/volcaniclastic sediments, covering several large areas: vent features (unit Tv), palagonitized tuff (unit Tpt), and pillowed lava flows. All of these volcaniclastic units are equivalent to or are parts of both the Tbas and Tbak lava flow units. All of the pyroclastic and pillowed units also contain minor lava flows. In most areas those intercalated flows are water affected.

The subaerial flow deposits of the Tbas and Tbak deposits are confined to the northern part of the Klamath Hills, where they overly both sedimentary deposits and palagonitic tuffs. Chemistry and petrography on samples of these units show that the predominant lithology is basaltic andesite, with secondary amounts of basalt and basaltic trachyandesite. The lack of age data or reliable stratigraphic markers makes correlation of these flows with other units in the area tenuous.

Tbak **Basaltic andesite of Klamath Hills (Pliocene or Miocene)—**Gray to dark gray, slightly to very slightly diktytaxitic, medium-grained basaltic andesite with no phenocrysts in hand sample, but numerous to abundant small groundmass plagioclase crystals. Visible olivine phenocrysts are very rare to none. The unit is the capping basalt on all of the ridges in the northern part of the hills, and its farthest south exposures are in the sections just to the north of the Township 40/41 boundary. In at least half of the exposures the lava flows have interacted in some way with water,

either by pillowing, or as water-affected flows. Some of the pillow deltas are quite thick, especially those in the gravel pits exposed at the south end of the "Folsom" ridge, in sec. 36, T40S, R9E. At the time of this report the over 300 feet of pillowed basalt in this area is being exploited on 3 different elevation levels. On the lowest elevation level the downfaulted pillow basalt has been mined back to the point that the adjacent white claystone is now exposed at the same elevation. The upper two levels both mine the original pillow delta, and in them it appears that the flows in the delta were flowing to the south. Another extensive area of pillowing is beneath the capping flows on the top of the "Short" ridge in sec. 21, T40S, R9E. Throughout the northern parts of the exposures of this unit, they appear to thicken to the east, but no vent area was found. All of the flows have been somewhat tilted by faulting from their original horizontal positions, so that they tilt gently away from the primary faults. Geochemically, the flows are basaltic andesite with 51-53 weight percent SiO_2 and ~16-17 weight percent Al_2O_3 (Table 1, map nos. 5, 37, 41, and 54). High loss on ignition (>3.5 percent) of the basaltic andesite at map no. 41 depresses the SiO_2 value to nearer 51 weight percent. High loss on ignition typically indicates alteration, such as would occur if the lava were water-affected. A comparison of the samples from this unit (Table 1, map nos. 37 and 54) with sample chips from the uppermost lava flow in the Ross well, KLAM 53769 (Table 1, map no. 41) show that they all have the same geochemistry. The Ross well is located in section 28, T40S, R9E. In the well log for that well, the uppermost solid lava flow was located between 82 and 87 feet below the ground surface. The lavas of that flow are overlain by clay and cindery deposits. Petrographically the samples of this unit do not contain phenocrysts, are slightly ophitic, have groundmass plagioclase crystals up to 2.0mm, and olivine crystals up to 0.75 mm, which show not alteration to iddingsite. One sample (Table 1, map no. 54) contains pyroxene crystals up to 1.0 mm. No dates are available for this unit, but its paleomagnetism is pretty consistently reversed. Thicknesses vary from a single flow of 2-3 m (6-10 ft), up to pillowed sections of over 30 m (100 ft)

Tbas **Basaltic andesite of Short (Pliocene and/or Miocene)—** Medium gray to black, fine grained to glassy, extremely hard, not diktytaxitic, basaltic andesite containing medium to large phenocrysts of plagioclase and varying amounts of medium olivine phenocrysts in hand sample. The unit is located throughout the northern part of the Klamath Hills. Stratigraphically, the flows of this unit are beneath the basaltic andesite of the Klamath Hills (unit Tbak), and are equivalent to or above the palagonitic tuff layers (unit Tpt). The flows of this unit exposed in the west-facing escarpment of the "Short" hill in secs. 20 and 21, T40S, R9E, appear to be unconformable with the overlying basaltic andesite unit (unit Tbak) and may also contain another, older unconformity within their section. This apparent unconformity and paleomagnetic readings of reversed as well as normal suggest that the flows of this unit may have been generated by more than one volcano, during more than one period of volcanic activity. One possible vent for the flows of this unit is discussed in the vent unit description (unit Tv). Both pillowed and water-affected flows are found within this section, but also exposed in the west escarpment of the "Short" hill are brecciated, highly cindery flows, perhaps aa in origin. In these aa flows the top and bottom breccias are each approximately 1.5 m (5 ft) thick, with a massive interior from 0.3-2 m (1-6 ft) thick of amygdaloidal basalt. Some flows within this unit contain clumps of plagioclase and olivine phenocrysts, but all contain the large to very large plagioclase phenocrysts that are found in most of the basaltic andesite units in this part of the Klamath Basin. Petrographically the plagioclase phenocrysts range in size from 0.5 mm to 3.25 mm. The olivine phenocrysts are not altered to iddingsite and range in size from 0.5-1.2 mm. Almost all of the samples contain black glass between the groundmass crystals, some of which has been altered to palagonite. Chemically, most of the samples of this unit (Table 1, map nos. 11, 19, 35, 36, and 40) fall within the basaltic andesite field (Le Bas and Streckeisen, 1991). This includes the sample from the uppermost flow in the Jones exploration well (Table 1, map no. 19, KLAM 53771). However, one sample, at map no. 40, falls within the basalt field. Another sample, at map no. 35 (Table 1), plots on the line between the basaltic andesite and the basaltic trachyandesite fields. This sample is from the lowest elevation flows exposed in the west-facing escarpment of the hill labeled

"Short". Thus, some variation exists among the lava flows mapped as the basaltic andesite of Short, and it seems that there may be some trend from the older basaltic trachyandesites to the younger basaltic andesites. In addition, the basaltic trachyandesite flows at map no. 35 have a normal magnetic polarity, while all of the other, and presumably younger, basaltic andesite flows have reversed magnetic polarities. In most areas the base of this unit is not exposed, but the greatest thickness that appears to be an unfaulted exposure is up to 275 m (900 ft)

Tv **Vent deposits (Pliocene and/or Miocene)**—Proximal red and gold cinder and breccia deposits and small lava flows. The unit is located in three areas in the southern part of the Klamath Hills, and in one place in the northwest corner of the Klamath Hills. All of the locations in the southern part of the area are related to, and are likely the eruptive centers for some of the extensive palagonitic tuff unit (unit Tpt) that is also located in that area. Most of the vent deposits have been exploited as cinder/gravel pits, but in one, the Farmers Rock Aggregate pit in sec. 5, T41S, R10E, the feeder for the pyroclastic vent area is being crushed for road aggregate. The geochemistry of a sample from this vent area, at map no. 55 (Table 1), is similar to the chemistry of samples of the basaltic andesite of Short (unit Tbas) exposed as subaerial units in the northern part the Klamath Hills. Petrographically, the rock also is similar to the basaltic andesite of Short (unit Tbas). It contains plagioclase phenocryst form 0.5-3.0 mm, and unaltered olivine phenocrysts up to 1.3 mm. Some of the abundant black glass, between the crystals in this sample, has been altered to palagonite. The most extensive cinder pits are located in and around the vent area located at the Merrill City Pits. The state, the county and the BLM road departments have all exploited this vent area for many years. Another possible vent area is located in sec. 1, T41S, R9E, and is much smaller than the other vent areas to the south. It consists of a single lava flow at the top of the hill, as well as a "rib" of basalt that crosscuts the underlying sedimentary layers. The flow is dark gray and fine grained and contains abundant visible plagioclase crystals. Neither the rib nor the small hill-capping flow contain any vesicles, which suggests that the flow may be a crater-filling flow, and that the "rib" may be the feeder dike for that small eruption. Finally, the vent in the northern part of the Hills is a red cinder pit located in sec. 17, T40S, R9E. The flows from this vent do not appear to have interacted with water. In fact, it appears that they are continuous with the lava flows to the south that can be seen in the lower part of the west facing escarpment of the tallest of the Klamath Hills, "Short" hill. Samples of the flows from this vent show a lithology with abundant small to medium plagioclase phenocrysts in clumps.

2.3 Tertiary volcanic and hypabyssal rocks at Stukel Mountain

Td **Hornblende dacite dike (Pliocene)**—Light-gray-weathering, light gray, fine-grained, hornblende dacite dike. Weathers to decimeter-sized tablets which break along vertical joints that trend N5-10E, parallel to the trend of the outcrop. Contact with the surrounding rocks is nearly vertical. Trachydacite in composition with ~66 weight percent SiO_2 and total alkalis (Na_2O and K_2O) exceeding 8 weight percent (Table 1, map no. 20). In thin section, comprised of 1-2 percent dark-green to black hornblende needles 1-7 mm long; 1-5 percent plagioclase phenocrysts 0.5-2 mm; in a groundmass of 65-75 percent microfelsite (feldspar and quartz <0.2 mm) 20-25 percent light-gray glass, and <1 percent extremely fine magnetite. The texture is hyalopilitic. Very limited in extent, the only exposure is found on the west flank of Stukel Mountain in sec. 9, T40S, R10E. Intrudes basaltic andesite (unit Tba)

Tmd **Mafic dikes (Pliocene)**—Brown-weathering, dark-gray, aphanitic dikes that intrude bedded palagonitic pyroclastic and sedimentary rocks at a high angle and disappear upward into the thick stack of basaltic andesite (unit Tba). These dikes are nearly vertical and sinuous being 1-2 m wide. Exposed on the west flank of Stukel Mountain in sec. 9, T40S, R10E Presumably basaltic andesitic in composition and interpreted to be feeder dikes for the upper lava flows at Stukel Mountain

Tba **Basaltic andesite (Pliocene)—**Mottled tan-orange to brownish-red and dark-gray-weathering, medium-dark-gray, slightly porphyritic, generally fine-grained basaltic andesite. Tabular to blocky in appearance, weathers to blocky angular talus on the steep slopes of Stukel Mountain. Basaltic andesite in composition with 52-55 weight percent SiO_2 and >17 weight percent Al_2O_3 (Table 1, map no.s 6, 7, 8, 9, 21, 22, and 24). In thin section consists of plagioclase 0.5-3 mm: 1-7 percent; 1-2 percent partially iddingsitized olivine generally <0.5 mm although rarely up to 1 mm; in groundmass of 40 percent feldspar microlites, 45 percent dark-gray glass, and 5 percent magnetite. Texture is usually moderately trachytic to hyalopilitic. New $^{40}Ar/^{39}Ar$ age of 4.25 ± 0.04 Ma (Table 2, map no. A4) from the summit of Stukel Mountain. This sample yielded a strongly U-shaped age spectrum with a minimum age of ~6.8 Ma without a plateau age. The total gas age of 23.5 ± 0.1 Ma was interpreted to be an overestimate of the eruptive age, because of excess argon. Fortunately the sample did yield a valid isochron, giving an age of 4.25 ± 0.04 Ma, and also substantiated that excess argon was present, with $^{40}Ar/^{36}Ar$ = 337. Thickness exceeds 305 m (1,000 ft)

Tbs **Basalt of Stukel Mountain (Pliocene)—**Mostly agglutinous lava, scoria, and scoriaceous vent agglutinate spatter. Consists of mottled red- and black-weathering, black or earthy red, fine-grained, basalt scoria and spatter, dark-gray to black-glassy scoria and cinders, and some dense, blocky and tabular flows. Vesicles 2-4 mm comprise 20-30 percent. Basalt in composition with <50 weight percent SiO_2 (map no.s 10, 23, 25, and 39). In thin section, scoria comprised of 5-10 percent partially iddingsitized olivine <0.5 mm; 30-40 percent plagioclase <1 mm; and 50-60 percent dark-reddish-gray to magnetite-bearing black glass. Texture is hyalophitic. Overlain by basaltic andesite (unit Tba). Bottom contact not exposed. Logs of a deep drill hole (KLAM 53527/53598, UTM NAD27 Zone 10 coordinates 4661787N, 611128E) spudded in agglutinous basalt of Stukel Mountain in NW¼ SW¼ sec. 9, T40S, R10E near the line of cross section A-A' indicate more than 210 m (700 ft) of predominantly cinders. Water in the hole was warm, but not hot, at 82º F. The drill hole data provides a local minimum thickness for the unit, 210 m (700 ft)

Tbav **Vent agglutinate, spatter, and cinders (Pliocene)—**Mottled reddish-brown and dark-gray, reddish-brown, vesicular, very-fine-grained basaltic andesite agglutinate. About 15 percent vesicles up to 1 mm. Chemically basaltic andesite and similar to unit Tba with which it is spatially associated. (Table 1, map no. 3). In thin section, comprised of 10 percent partially iddingsitized olivine <0.3 mm; 30-40 percent plagioclase <0.5 mm; 50-60 percent black glass. Texture is hyalophitic. Small exposure located in sec. 16, T40S, R10E.

2.7 Tertiary volcanic rocks in cross section only

Tbu **Basalt and basaltic andesite (Miocene)—**Mainly lava flow rocks but also pyroclastic rocks as deduced by geophysical means and penetrated by deep wells drilled in 2001 by the California Department of Water Resources in the Tule Lake Basin to the east near the Oregon-California border.

3.0 STRUCTURE

The map area lies within the Klamath basin, which is at the juncture of the Cascade Range and Basin and Range physiographic provinces. The Klamath Hills, Stukel Mountain, and the surrounding valleys lie within the extensional Basin and Range tectonic province that dominates the physiography of the state of Nevada, and extends into southern Idaho and south-central Oregon. The overall grain of the structure mimics the general geomorphic trends of the Basin and Range province--large, north-to-northwest trending graben valleys, separated by large horst mountain blocks. The southwest to northeast cross section A-A' shows this horst and graben pattern with volcanic rocks dominating in the mountain highlands and thick sediments, determined by geophysical means (French and others, 2003), in the graben

valleys. Offsets along faults are in the range of hundreds of feet or more. Offset on the range-bounding zone of faults on the west side of the Klamath Hills may have as much as 1,000 m (3,000 ft) of throw (Northwest Geophysical Associates, Inc., 2002). Near some of the faults, volcanic units, particularly pyroclastic units, have been deformed producing drag folds—the principal cause of high-angle dips in the map area.

The Hamaker Mountain-Chase Mountain volcanic edifice is considered part of the Cascade Range (Mertzman, 1996). Hamaker Mountain and its ancillary peak, Chase Mountain, is a compound shield volcano. Several northwest-trending normal faults with significant offset bisect the volcanoes. The most pronounced fault is the herein named Bear Valley Fault. Marker horizons are not found in the lava flows at Hamaker Mountain and Chase Mountain, but the eastern Bear Valley escarpment gives an indication of the minimum throw along the fault, rising up to 150 meters (500 feet) above the valley floor.

In the foothills along the southern margin of Hamaker Mountain, normal faults provide topographic and structural relief where Miocene volcanic rocks are exposed, including the basalt of Grenada Butte (unit Tbg) and the megacrystic basalt (unit Tbm). These Miocene volcanic rocks are the foundation upon which the volcanic highlands of Hamaker Mountain and Chase Mountain were built. East-west trending faults are also found cutting the highlands between Grenada Butte and Hamaker Mountain, but their effect upon the area's geomorphology, although significant, is less pronounced.

Immediately east of the Hamaker Mountain-Chase Mountain highlands is a complex graben, herein named the Lower Klamath Lake Graben (Figure 8). It is similar to the Klamath Falls Graben defined by Blakely and others (1997), north of Klamath Falls because (1) its valley has been occupied by a lake in historical time, (2) it is structurally complex (multiple internal faults and at least one horst within it, and (3) it occupies a gravity low. Several geophysical surveys conducted by various firms in 2001, as part of groundwater exploration studies in the Klamath Drainage District (KDD), provided structural information about the graben. Since there are few wells in the KDD, the main objective of these surveys was to map both the depth to volcanic basement and the intrabasinal fault zones. Defining the subsurface was intended to be used for locating attractive targets for irrigation well drilling, particularly fault-zones with fractured lava flows or porous basaltic tephra.

Northwest Geophysical Associates, Inc. (NGA) integrated three different geophysical surveys within the KDD to develop their structural geologic model of the subsurface of the Lower Klamath Lake

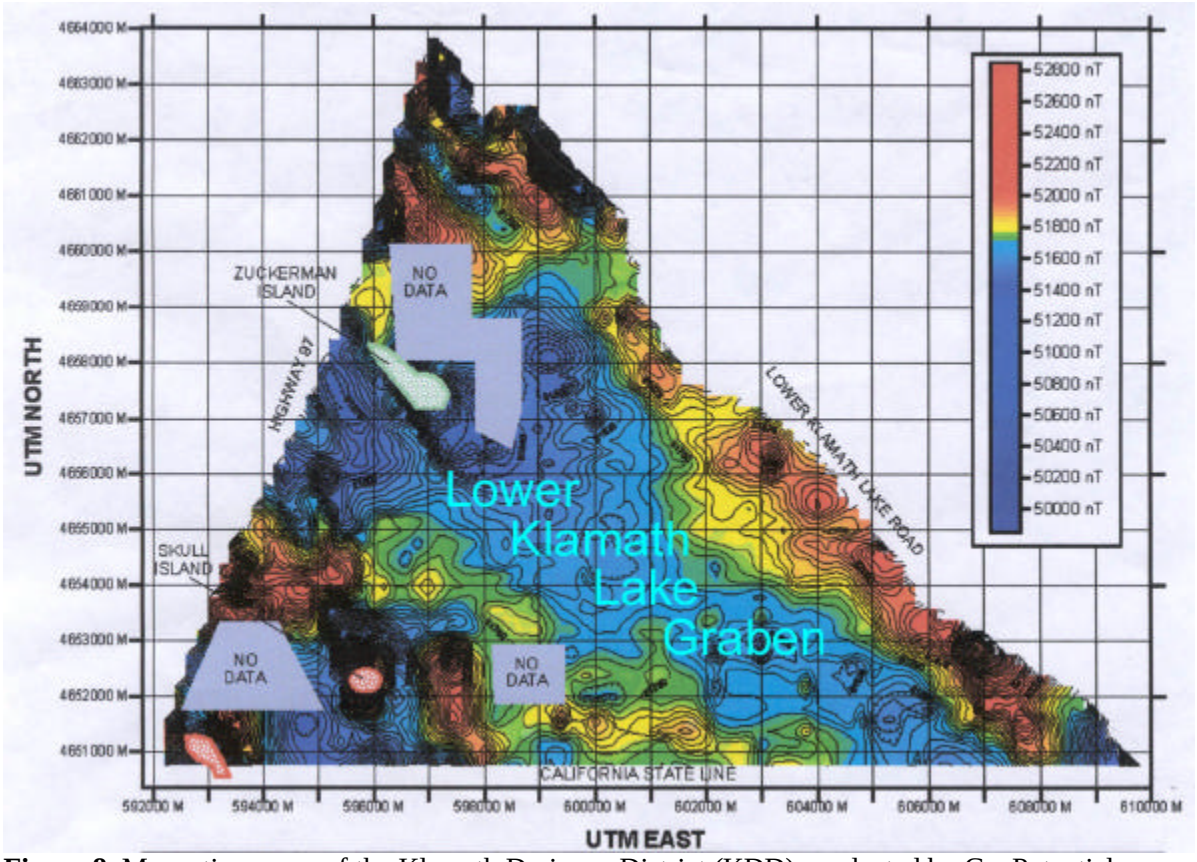

Figure 8. Magnetic survey of the Klamath Drainage District (KDD) conducted by GeoPotential Environmental and Exploration Geophysics in 2001.

basin (Figure 9). The surveys used were a "terramagnetic" survey conducted by GeoPotential, NGA's own gravity survey of approximately 200 stations, and three 2-km-long seismic reflection lines done by Cooksley Geophysical of Redding, CA. From these data NGA interpreted an east-west cross section beginning at Highway 97 and extending eastward to the base of the Klamath Hills. Their line passes a short distance north of Zuckerman Island. The data indicate horst and graben patterns in the subsurface of the northern part of the Lower Klamath Lake Graben (Northwest Geophysical Associates, Inc., 2002; French and others, 2003). Near the Klamath Hills there are 500-600 m of lacustrine sediments overlying the interpreted volcanic basement. This geophysical interpretation provides control for sediment thicknesses near the Klamath Hills for this study's cross section, A-A'. NGA's cross section also shows the Zuckerman Island horst bifurcating the northern part of the Lower Klamath Lake Graben. The internal horst-and-graben complexity of the graben, however, diminishes in the southern part of the valley near the California border, where thicknesses of the basin-fill sediments and pyroclastic tuffs increase to as much as 1,000 meters (3,000 feet) (Northwest Geophysical Associates, Inc., 2002).

Unexposed, intrabasinal faults in the Klamath Drainage District (KDD), shown in pink on the geologic map were interpreted by integrating surface geology, magnetics (Figure 9), and integrated magnetics and gravity (Figure 8). Some of the intrabasinal faults that were identified geophysically are continuous with faults exposed at the surface, such as those at Wild Horse Butte. The geometry of exposed fault planes at the surface influences our interpretation of faults in the subsurface. Geophysicists interpreted faults along linear bands of magnetic and gravity contrasts. Less magnetic areas are generally toward the basin, and, therefore, fault offset is interpreted to have the downthrown block on the less magnetic side. GeoPotential's interpretation shows fault lines with jagged angles (Figure 10). Our interpretation smooths the fault lines, because the faults exposed at the surface in the Klamath Basin generally have more smooth, curvi-planar traces. Circular faults and right-angle bends in faults are generally not favored based upon our geologic mapping. Instead, right-angle bends in faults are usually due to the presence of cross faults.

Within the Lower Klamath Lake Graben two small "islands" of rock poke through the virtually horizontal valley-filling sediments. Skull Island is an erosion-resistant volcanic butte. Zuckerman Island is a horst (Northwest Geophysical Associates, Inc., 2002; French and others, 2003), which continues northwest to include Wild Horse Butte. The horst is bounded on the west by the Wild Horse Butte Fault and on the east by the Zuckerman Island Fault. The plane of the northwest-trending Wild Horse Butte

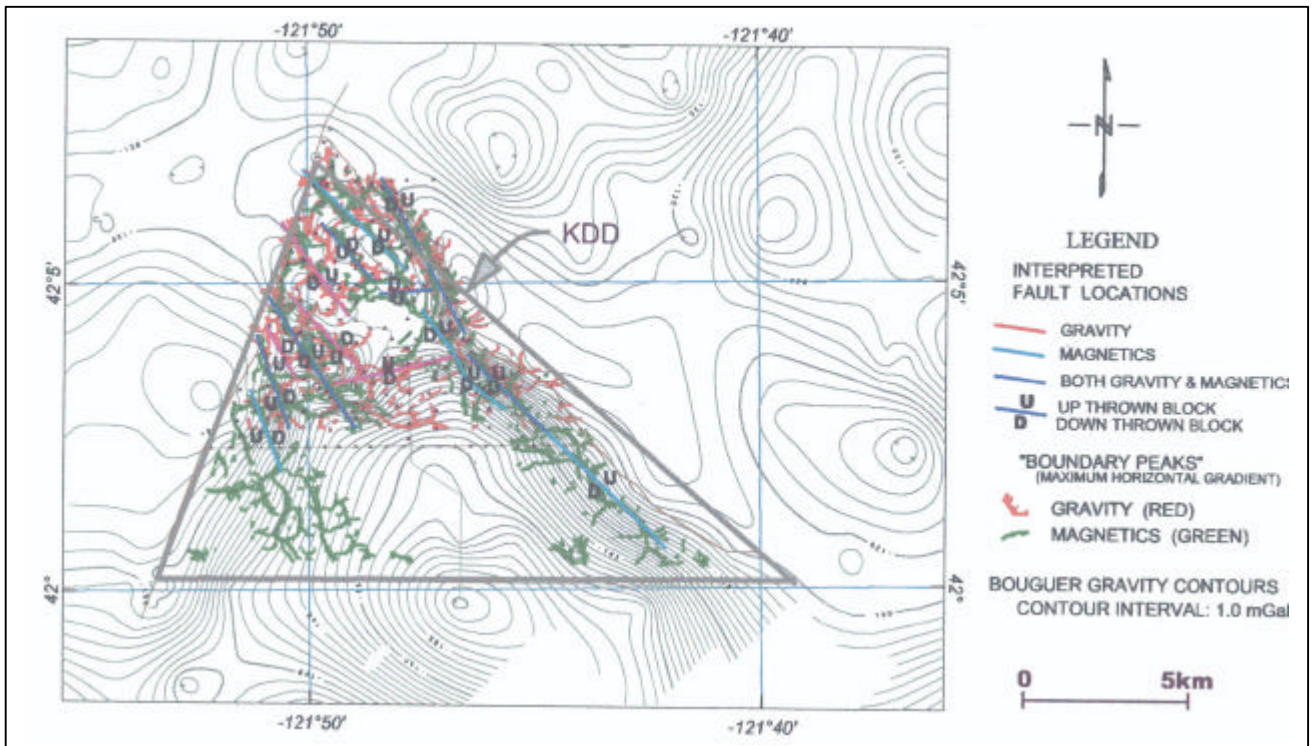

Figure 9. Integrated geophysical model of the subsurface structure of the Klamath Drainage District as developed by Northwest Geophysical Associates (French and others, 2003).

Fault is exposed within the Flowers Quarry in sec. 23, T40S, R8E. Interestingly, the fault surface is slightly curvi-planar, not only in its strike direction but also in the dip direction. Measured dips on this smooth, nearly polished fault surface range from 59°-67°. Slickensides parallel the dip direction with no apparent obliqueness. Because the Wild Horse Butte Fault and other exposed normal faults in the Klamath Basin have similar dip angles, it is assumed that faulting within the map area is principally high-angle normal faulting of the Basin and Range type.

The Lower Klamath Lake Graben is bounded on the east by the Klamath Hills—a large, complex, northwest-trending horst block. Within the Klamath Hills horst are numerous smaller, fault-controlled ridges. Most of these ridges are the result of movement on north to northwest-trending normal faults that mimic the predominant north/northwest trending Basin and Range faulting. However, these faults are all cut by several major east-west trending faults that incrementally drop the units down almost 300 meters (1,000 feet) in elevation to the valley floor. Similar east-west displacements offset the northwest-southeast faulting in the Lost River Valley east of the Klamath Hills. However, these faults are more difficult to document and trace laterally because of the subsequent erosion of the older sediments and the newer valley fill from Lost River fluvial deposition. It is possible that some of these east-west faults may have some oblique strike-slip movement, but that movement is difficult to document.

Much of the southern part of the Klamath Hills does not appear to have the same amount of faulting as is found in the northern part. It is possible that this discrepancy is the result of the erosion and weathering patterns of the softer pyroclastic and sedimentary units. The lack of ridge-forming lava flows in this area likely obscures the presence of faults that would otherwise be more apparent. In addition to the offset of the volcanic units by the faulting in the area, the movements on the faults have also tipped the flows so that they dip between 1 and 5 degrees. While the dip is not always consistent in a particular direction, it does appear that more of the capping lava flows on the ridges dip down to the west and southwest than in any other direction.

East of the Klamath Hills is a graben occupied by the valley of the Lost River. Like the valley west of the Klamath Hills, it is tectonically controlled and internally complex. It differs, however, in that it has not been occupied by a lake during Holocene time, and thus, does not have the nearly horizontal topographic expression found in the Lower Klamath Lake Valley. This eastern valley contains numerous smaller horsts and grabens that break up the surface of the valley floor.

Stukel Mountain is a center of volcanic accumulation, uplifted along two major west-dipping faults: the Stukel Mountain Fault and the Upper Stukel Mountain Fault. Uplift of the west side of Stukel Mountain has, in general, tilted strata eastward. Stukel Mountain is part of a complex horst block that extends into the Dairy, Merrill, and Malin quadrangles (Hladky, 2003; Jenks and Madin, 2003). Where these two faults cross Quaternary alluvial fan deposits, subtle scarps provide evidence of Quaternary movement, at least on some fault segments.

The age of the onset of faulting here is just as problematic as it is within the rest of the Klamath Basin. Some geologists (Peterson and McIntryre, 1970; Sherrod and Pickthorn, 1992) have suggested that the onset of major Basin and Range faulting in this region was Pleistocene, or perhaps late Pliocene. Other authors (Hart, and others, 1984; Black, 2004; Murray, in press,) postulate a much older 7-Ma or Miocene age for the onset of the predominant north/northwest-trending, high-angle Basin and Range faulting.

The interplay between faulting and volcanism, occurring penecontemporaneously over a broad time span, makes deciphering the age of the onset of faulting difficult. Propagating rifts probably controlled the initial extrusion of lava to the surface. The dikes and chains of volcanic vents, which source the volcanic accumulations, are sensitive indicators of extension direction in the Basin and Range province (Zoback and Thompson, 1978). The volcanic units in the mapped area span a range of ages from Miocene at Grenada Butte, to early Pliocene at Stukel Mountain, to late Pliocene at Hamaker Mountain and Chase Mountain. Units of all ages are disrupted by faulting, which has probably occurred episodically along many of the same faults.

Several factors indicate that extension has been intermittently continuous to the present day. Quaternary alluvial fans show visible (in air photos) linear offsets at Stukel Mountain. At the Flowers Quarry at Wild Horse Butte, secs. 22 and 23, T40S, R8E, smooth fault planes both cut and entrain colluvium in the fault gouge. Similarly, in the gravel pit in sec. 8, T40S, R9E, of the Klamath Hills it is possible that the exposed fault offsets colluvium of unknown age and actually drags it down within the fault surface. Finally, the West Klamath Lake fault zone (Bacon and others, 1999), northwest of Klamath Falls, generated the Klamath Falls earthquakes of 1993 (Wiley and others, 1993). The relatively young, undissected appearance of the major fault scarps, and the complete lack of established streams within much of the mapped area, indicate that the most recent movements on the major northwest-trending faults that formed the highlands vs. the valleys are relatively young. All of these facts point toward continuing seismicity due to Basin and Range extension.

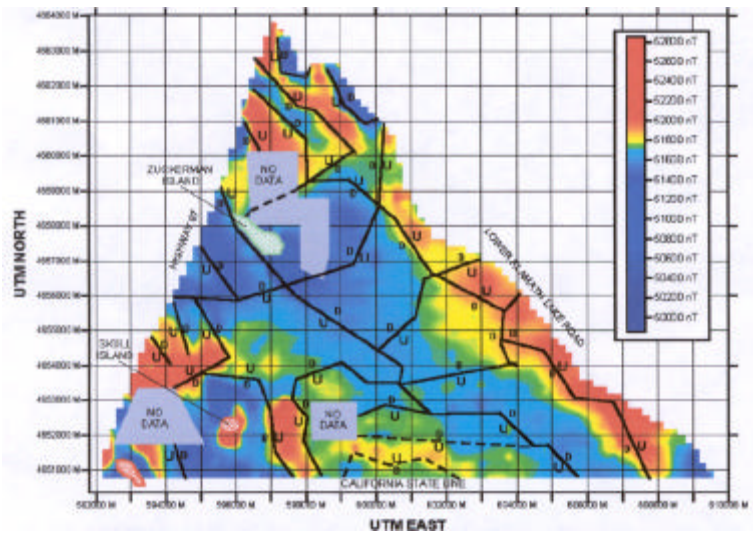

Figure 10. Intrabasinal faults within the KDD as interpreted by GeoPotential.

There is no geophysical data for the valley of the Lost River. Selected wells, however, in the Lost River valley near the line of cross section A-A', notably the Walsh well (KLAM 52697) and the Peacore well (KLAM 53527/53598), provide control for the subsurface geology. The Walsh well indicates sediment thicknesses of more than 120 m (400 feet) beneath the Lost River valley floor. The Peacore well, which spuds in cinders and agglutinous lavas, indicates a wedge of cinder-dominated lava more than 210 m (700 feet) thick near the base of Stukel Mountain (see cross section A-A' for graphical interpretation).

4.0 GEOLOGIC HISTORY

The geologic history of the area begins in Miocene time with the deposition of palagonitic tuff (unit Tpt).These deposits are the result of explosive surges from lava-water interactions in vent areas, and are coeval with the deposition of fine-grained sediments (unit Tms), mostly in lacustrine environments. Subsequently, about 6 Ma, basalt lava erupted into a water-rich environment, probably lakes and marshes, and the lava flows were altered to the water-affected basalt of Grenada Butte (Tbgw). As these basalt flows displaced surface water in the area, they accumulated unaltered as the basalt of Grenada Butte (unit Tbg). The basalt of Grenada Butte may have erupted from a series of vents, but we have little information about their spatial distribution. Only one is exposed today (unit Tbgv). These basalt eruptions constructed local relief—which provided the gravitational potential necessary to generate lahars (unit Tbgl). Slightly before the eruption of the basalt of Grenada Butte, the underlying megacrystic basalt (unit Tbm) likely erupted onto dry ground (at least none of the sections currently exposed are water-affected). Its isotopic age is approximately that of the basalt of Grenada Butte. The precision of the basalt ages (Tbm <5.89 Ma and Tbg = 6.15 ± 0.17 Ma) is equivocal and very nearly equivalent. Thus, we surmise that the geologic history, as reflected in units exposed at the surface, begins with the deposition of fine-grained, primarily

lacustrine sediments in a late Miocene basin, coeval basaltic eruptions through water-saturated sediments and/or standing water that produced palagonitic tuffs, followed by lava flows onto dry ground. Black (2004) surmises that this initial basin sedimentation followed as a result of extensional rifting beginning about 7 Ma. The pre-7-Ma basement exposed to the west of the Klamath Basin consists of calc-alkaline volcanic rocks, mainly lava flows (Smith and others, 1982; Fiebelkorn and others, 1983; Mertzman, 1996; Mertzman, 2000).

The recurring events of late Miocene and Pliocene time are that sediments continued to be deposited into tectonically extending basins, and basaltic eruptions through water-saturated sediments continued to produce pyroclastic surges that deposited palagonitic tephra. Although our age control is poor for the flows in the Klamath Hills and the base of Stukel Mountain, we recognize this pattern of the geology beginning with the lowest exposed Miocene rocks near Worden and capped by 4-Ma Pliocene flows at Stukel Mountain. Sometime in Pliocene time, basaltic andesite erupted (unit Tbpb) and intruded (unit Tbaw) at Pearson Butte and flowed out onto the areas of what is now Wild Horse Butte (unit Tbwb) and was water-affected in the area of the present-day Lake Miller (unit Tblm).

In the Klamath Hills, basaltic andesite lavas erupted through sediments, producing palagonitic tuffs. Following, but perhaps in part at the same time as the eruption of the palagonitic tuff deposits, the flows of the basaltic andesite of Short (unit Tbas) began to cover the northern part of the palagonitic tuff terrain. These flows were cindery at their vents, and were "sticky" enough that some may have formed aa-type flows. At least one apparent unconformity within the section of the basaltic andesite of Short suggests that some tectonic activity may have happened during the period of time during which the entire stack of flows was erupted.

In at least a couple of areas, exposures of sediments above the basaltic andesite flows suggest that a period of hiatus may have occurred between the eruption of these flows and the eruption of the overlying basalt andesite flows of the Klamath Hills (unit Tbak). In addition, a number of areas within the lower part of this basalt unit are extensively pillowed, which indicates that they were erupted into some body of water. In at least two places fish fossils in the intervening sediments between the basaltic andesite flows of Short and the basaltic andesite flows of the Klamath Hills suggest that the body of water may have been lacustrine. Most of the upper parts of this unit, however, are made up of subaerially emplaced flows, which suggests that the lake environment did not last through the entire eruptive cycle, or perhaps that the lakes during the later eruptions were confined to smaller areas than the preceding lake that received the palagonitic tuff. One very interesting exposure of well-rounded gravels at a pit located in sec. 23, T40S, R9E, suggests that the younger flows may have also been associated with fluvial environments.

The history at Stukel Mountain begins with basalt flows and cinders (unit Tbs), largely unaffected by water. These flows and cinders were overlain by local palagonitic tuffs, which were intruded by mafic dikes. Subsequent voluminous basaltic andesite flows (unit Tba) capped the Stukel Mountain sequence. Isolated pockets of these flows, a few tens of square meters is size, are palagonitized and cindery. The capping lavas are early Pliocene age (4.25 ± 0.21 Ma, Table 2).

In late Pliocene time, slightly less than 3 Ma, the eruption of alkaline basaltic trachyandesite lavas heralded the beginning of Hamaker Mountain. Some of these lava flows travelled several miles and are exposed in the canyon of the Klamath River west of Keno (Hill, 1996; Hladky and Mertzman, 2002). They were followed shortly by voluminous basaltic andesite eruptions that built the Hamaker Mountain edifice. This volcanism then shifted northward and built the Chase Mountain shield and blanketed areas eastward to the Klamath River. About 2 Ma, deep-sourced tholeiitic basalt erupted from undiscovered fissures—the basalt of Keno (Hill, 1996; Hladky and Mertzman, 2002). The fluid basalt of Keno filled canyons and valleys along the base of Chase Mountain.

Our limited age data indicate that the thickest volcanic accumulations took place in Pliocene time. Volcanic accumulations in what are now the modern highlands of Hamaker Mountain, the Klamath Hills, and Stukel Mountain ultimately were substantial—lava flows accumulated from hundreds to thousands of feet thick. In contrast, volcanic activity in the valley floors was generally limited and meager. Our lack of age data and contiguous stratigraphic relationships makes it difficult to pinpoint the age of these smaller eruptions. Suffice it to say, that in the valley west of the Klamath Hills, small basaltic andesite eruptions produced the cinder cone and lava flows at Horsehead Island. Thin, cindery and agglutinous lavas erupted

over water-saturated sediments at Lake Miller and Zuckerman Island. Some of the volcanism may have been fed along intrabasinal structures, such as the faults that bound the Zuckerman Island horst. Small andesite eruptions produced agglutinate, blocky flows, and water-affected lava at Skull Island. In the valley east of the Klamath Hills, there are no plugs or cinder cones, although this area did undergo small-scale horst and graben extension, some of which has continued to Quaternary time. The southern part of the Klamath Hills underwent somewhat greater extension than the northern part (Northwest Geophysical Associates, Inc., 2002) but accumulations of erosion-resistant capping volcanic flows were replaced with the eruption from several vents of palagonitic tuff.

As the two valleys on either side of the Klamath Hills formed, sedimentation continued, and the valley-fill sediments, both Quaternary/Tertiary in age (unit QTs) and, subsequently, Quaternary in age (unit Qs, unit Qhl) were deposited. On the western side of the Klamath Hills the sedimentation (unit Qhl) was dominated by the presence of Lower Klamath Lake. What is now the Klamath Drainage District (KDD), was drained in the 1920's and 1930's for agricultural purposes (French and others, 2003). Nearshore sand and dune deposits on the shores of the lake have since been redistributed by wind deposition, such as at Lake Miller and White Lake (unit Qe). Several of the more incised draws in the area, such as the Captain Jack draw deposited sediments in alluvial fans (unit Qaf) along the shores of Lower Klamath Lake. Alluvial fans (unit Qaf) coalesced forming a bajada on the west flank of Stukel Mountain. And today, within their floodplains the Lost and Klamath Rivers are both eroding and depositing alluvial sediments.

On the eastern side of the Klamath Hills a mixed environment of a number of shallow, perhaps annual, lakes and the fluvial sedimentation of the Lost River resulted in more diverse sedimentary structures and relationships than on the west side which was dominated by lacustrine sedimentation. It is puzzling, however, that well logs east of the Klamath Hills, do not contain any significant thicknesses of pebble and cobble gravel (Appendix E). This lack of coarse sediment indicates that the Lost River was probably not carrying much load and may have meandered more in the past than its present course would suggest. Modern lacustrine sedimentation continues in the shallow lakes that are used for irrigation drainage and storage.

5.0 GEOLOGIC RESOURCES AND HAZARDS

5.1 Surface and ground water resources

Springs are rare in the map area. There are no springs in the upland areas surrounding Hamaker Mountain and Chase Mountain. At best, there are seasonal seeps. Despite the presence of "Spring" Lake at the north end of the Klamath Hills, no active springs were found within the area of the Klamath Hills. However, the mapping was completed during a period of drought. Thus, seasonal springs that may flow during more normal rainfall years were not flowing at the time of the field work for this report. The ranchers in the area have built numerous small reservoirs to contain runoff. These reservoirs are used to either supplement irrigation water from wells and the Lost River, or to water cattle herds. One spring is located on Stukel Mountain in the northeast corner of the map in sec. 3, T40S, R10E. It supplies water to a stock pond and its flows decrease to almost nil during the late summer.

The area of the Lost River Valley to the east of the hills has hundreds of domestic wells that have been drilled to varying depths over the years (Appendix E). In the past three years a number of irrigation wells have also been drilled with varying amounts of success. In most cases the successful wells have been drilled near the valley wall fault escarpments, or on the small horsts within the valley floor. The principal aquifers for the domestic wells are the black, basaltic sand and cinder layers that are within the thick sediment section. Successful irrigation wells hit either the basalt/basaltic andesite aquifer at a shallow depth, or hit one of the bounding faults of the Klamath Hills. Even short distances away from the bounding faults can mean a difference between hitting the basalt aquifer at 60 m or less, or drilling 300 m or more of fine-grained sediments.

Most of the wells that have been drilled in the map area are domestic wells for farm and ranch houses located near the valley floor. In contrast, the wells southeast of Keno are for residences on small acreages. In the southern part of the Klamath Hills and near Wild Horse Butte ranchers have drilled a few

irrigation-type wells. During the fall and winter, 2002-2003, the Klamath Hills Irrigation District drilled 8 exploration wells along the west side of the Klamath Hills to test the potential for further developing the aquifer. No irrigation wells have ever been successfully drilled in the floor of the Lower Klamath Lake valley. The geophysical studies (French and others, 2003) of the valley floor suggest that a few areas might be targets for drilling, but even those areas would have to drill 150-300 meters (500-1,000 feet) of fine-grained sediments before reaching the basalt aquifer. Thus, it is unlikely that exploitation of that aquifer will happen in the near future.

5.2 Gravel and aggregate resources

The proximity of the map area to the greater Klamath Falls area makes it an excellent resource for the gravel and aggregate needs of the local towns and agricultural community. Aggregate sites are shown on the map. Five of the pits are large and were being actively commercially mined at the time of this report. These pits are: the Farmer's Rock Aggregate Pit in sec. 5, T41S, R10E; the O'Connor West Pit in sec. 36, T40S, R9E; the Merrill City Pits in sec. 10, T41S, R10E; the Flowers Quarry at Wild Horse Butte, secs. 22 and 23, T40S, R8E; and the Keno Rock Pit at Horsehead Island, sec. 4, T40S, R8E. A large, inactive quarry at the north end of Stukel Mountain in sec. 5, T40S, R10 E. shows evidence of reclamation recontouring of some of its highwalls. It was not active during the period of mapping. At the Farmer's Rock Aggregate pit the operators are mining the central vent area of a volcano, which includes pillowed basalt, dike materials from the central vent dike, and some pyroclastic tuff. At the Merrill City Pits and the nearby State/BLM Pits the operators are exploiting the palagonitic basaltic tuff and some of the central parts of the volcanoes that erupted the tuff. At the O'Connor West Pit three separate levels of pit access pillow basalt, both on the footwall, and in the downfaulted block of the same unit. At the Flowers Quarry, agglutinous and tabular basaltic andesite lavas are being exploited. Some gravel-rich colluvium on the footwall of the Wild Horse Butte Fault is being exploited, too. The operation at the Keno Rock Pit exploits black cinders and thin, interbedded (<2 m) basaltic andesite flows. All of the other pits in the Klamath Hills area are much smaller and are only sporadically mined by the local agricultural community for a number of applications.

5.3 Geothermal resources

In one area of the Lower Klamath Lake Road, on the west side of the Klamath Hills, groundwater temperatures are sufficiently high to be used for geothermal heating. The area of geothermal water appears to be associated with the main valley-bounding fault that separates the Lower Klamath Lake graben from the Klamath Hills horst. In particular the area of geothermal temperatures in the domestic and irrigation wells is in secs. 27, 28, 34, and 35 in T40S, R9E and secs. 1 and 2 in T41S, R9E. Many wells have temperatures in the 80^{o}-90^{o} F. range (Appendix E), but a few wells have temperatures in the 120^{o}-190^{o} F. range and one even reaches 200^{o} F. The geothermal water is both helpful and a hindrance to the local farmers and ranchers. The Liskey Farms in sec. 34, T40S, R9E use the geothermal water to heat extensive greenhouses that sell nursery plants to gardeners in the Klamath Falls area. They also raise exotic tropical fish for pet stores. However, the water is so hot that it must be cooled for even these purposes and is therefore nearly unusable for irrigation or stock water purposes. During the water crisis of the summer of 2001 several of the ranchers developed systems to cool the water, and then irrigated some pastureland with it. However, the water also contains various salts and heavy metals that make it unsuitable as a long term source of irrigation water.

In 1976 the Thermal Power Company drilled a geothermal exploration well in sec. 35, T40S, R9E (Appendix B). The bottom depth was 5,842', but temperatures were not above the range that might be expected for groundwater at such depths. This data makes it even more likely that the geothermal water in the area is connected to the valley-bounding faults and not to some large geothermal aquifer that simply surfaces in one particular area.

An examination of water temperatures from wells on the western flank Stukel Mountain indicates local geothermal influences. The Walsh well (KLAM 52697) in sec. 8, T40S, R10E produced 80^{o} F-water from a depth of 105 feet. The Peacore well (KLAM 53598) in sec. 8, T40S, R10E encountered 82^{o} F-

water at a depth 448 feet (Appendix E). In contrast, water temperatures for wells on the west side of the map area, along the Keno-Worden road and south of Worden, are cool: 40^{o}-60^{o} F.

5.4 Earthquake and mass wasting hazards

No earthquakes have been reported in historical times centered within the mapped area. However, numerous Quaternary faults dissect the area, some of which are new to those delineated previously by Hawkins and others (1989) and Sherrod and Pickthorn (1992). The earthquake potential for the region was demonstrated on September 20, 1993 when a foreshock with Richter magnitude 3.9 was followed by a magnitude-5.9 shock and a magnitude-6.0 earthquake (Wiley and others, 1993). Aftershocks continued for several months. The seismicity was located northwest of Klamath Falls along the West Klamath Lake fault zone, which is capable of generating 6.0 to 7.3 magnitude earthquakes (Bacon and others, 1999). The Klamath Falls region is recognized as one of Oregon's principal areas for damaging earthquakes (Madin and Mabey, 1996).

Hazards related to earthquakes in the map area include ground movement and mass wasting movements, either as slides or large block rockfalls. No historical landslides were encountered or seen on aerial photos during the field work for this mapping project. However, the presence of large blocks of basalt at the base of the hill called "Short" along the Lower Klamath Lake Road suggests that rockfall from normal erosion or from seismic events has happened in the past. Given the history of seismic activity in the Klamath Basin area, it seems likely that similar earthquake-generated rockfalls and ground movements will happen in the future.

6.0 ACKNOWLEDGEMENTS

This mapping was supported in part by the U.S. Fish and Wildlife Service under assistance award #11450-1-J513. The authors are grateful to the ranchers and landowners throughout the mapped area for their permission to survey their lands. Our thanks to the staff geologists of the Oregon Department of Geology and Mineral Industries for their discussions and in-the-field observations.

The views and conclusions contained in this document are those of the authors and should not be interpreted as necessarily representing the official policies, either expressed or implied, of the U.S. Government.

Field work conducted during the Spring, Summer, and Fall of 2002

7.0 REFERENCES

Adam, D.P., Rieck, H.J., McGann, M.L., Schiller, K.H., and Sarna-Wojcicki, A.M., 1995, Lithologic description of a sediment core from Round Lake, Klamath County, Oregon: U.S. Geological Survey Open-File Report 95-0033, 49 p.

Bacon, C.R., Lanphere, M.A., and Champion, D.E., 1999, Late Quaternary slip rate and seismic hazards of the West Klamath Lake fault zone near Crater Lake, Oregon Cascades: Geology, v. 27, p. 43-46.

Bates, R.L, and Jackson, J.A., 1987, Glossary of geology, third edition: Alexandria, Va., American Geological Institute, 788 p.

Black, G.L., 2004, Geologic map of the Lorella quadrangle, Klamath County, Oregon: Oregon Department of Geology and Mineral Industries Open-File Report O-04-07, scale 1:24,000.

Blakely, R.J., Christiansen, R.L., Guttanti, M., Wells, R.E., Donnelly-Nolan, J.M., Muffler, L.J.P., Clynne, M.A., and Smith, J.G., 1997, Gravity anomalies, Quaternary vents, and Quaternary faults

in the southern Cascade Range, Oregon and California: Implications for arc and back-arc evolution: Journal of Geophysical Research, v. 102, p. 22,513-22,527.

Cebula, G.T., M.J. Kunk, H.H. Mehnert, C.W. Naeser, J.D. Obradovich, and J.F. Sutter, The Fish Canyon Tuff, a potential standard for the 40Ar-39Ar and fission-track dating methods (abstract), Terra Cognita (6th Int. Conf. on Geochronology, Cosmochronology and Isotope Geology), 6, 139, 1986.

Fiebelkorn, R.B., Walker, G.W., MacLeod, N.S., McKee, E.H., and Smith, J.G., 1983, Index to K-Ar determinations for the State of Oregon: Isochron/West, no. 37, p. 1-60.

French, R. B., Jenks, M. D., and Connard, G. G., 2003, Geophysical investigations for groundwater in the Lower Klamath Lake basin, Oregon: Symposium on Applications of Geophysics to Engineering and Environmental Problems, Paper GWT01, 12 p.

Hart, W.K., Aronson, J.L., and Mertzman, S.A., 1984, Areal distribution and age of low-K, high –alumina olivine tholeiite magmatism in the northwestern Great Basin: Geological Society of America Bulletin, v. 95, p. 186-195.

Hawkins, F.F., Foley, L.L., and LaForge, R.C., 1989, Seismotectonic study for Fish Lake and Fourmile Lake Dams, Rogue River Project: U.S. Bureau of Reclamation Seismotectonic Report 89-3, 26 p.

Hill, M., 1996, The geochemistry and petrogenesis of volcanic rocks near Keno, Oregon, in the Southern Cascade Range, in: Manduca, C.A., and Mankiewicz, C., eds., Ninth Keck Research Symposium in Geology, abstracts volume, p. 192-195.

Hladky, F. R., 1998, Age, chemistry, and origin of capping lava at Upper Table Rock and Lower Table Rock, Jackson County, Oregon: Oregon Geology, v. 60, no. 4, p. 81-91.

Hladky, F. R., 2003, Geologic map of the Dairy quadrangle, Klamath County, Oregon: Oregon Department of Geology and Mineral Industries Geologic Map Series GMS–112, scale 1:24,000.

Hladky, F. R., and Mertzman, S. A., 2002, Geologic map of the Keno quadrangle, Klamath County, Oregon: Oregon Department of Geology and Mineral Industries Geologic Map Series GMS–102, scale 1:24,000.

Irvine, T.N., and Baragar, W.R.A., 1971, A guide to the chemical classification of the common volcanic rocks: Canadian Journal of Earth Sciences, v. 8, no. 5 p. 523-548.

Jenks, M.D., 2004, Geologic map of the Bryant Mountain and Langell Valley quadrangles, Klamath County, Oregon: Oregon Department of Geology and Mineral Industries Geologic Map Series GMS-117, scale 1:24,000.

Jenks, M.D., and Bonnichsen, B., 1989, Subaqueous basalt eruptions into Pliocene Lake Idaho, Snake River Plain, Idaho in Chamberlain, V.E., Breckenridge, R.M., and Bonnichsen, B., eds., Guidebook to the Geology of Northern and Western Idaho and Surrounding Area: Idaho Geological Survey Bulletin 28, p. 17-34.

Jenks, M.D., Bonnichsen, B., and Godchaux, M.M., 1998, Geologic map of the Grand View-Bruneau area, Owyhee County, Idaho, digitally compiled version: Idaho Geological Survey Technical Report 98-1, scale 1:100,000.

Jenks, M.D., and Madin, I.P., 2003, Draft geologic map of the Merrill and Malin quadrangles, Klamath County, Oregon: Oregon Department of Geology and Mineral Industries Open-File Report O-03-03, scale 1:24,000.

Le Bas, M.J., and Streckeisen, A.L., 1991, IUGS systematics of igneous rocks: Journal of the Geological Society (London), v. 148, p. 825-833.

Madin, I.P., and Mabey, M.A., 1996, Earthquake hazard maps for Oregon: Oregon Department of Geology and Mineral Industries Geological Map Series GMS–100.

Mertzman, S.A, 1996, Late Tertiary Cascades volcanism in the area west of Klamath Falls, Oregon: in: Manduca, C.A., and Mankiewicz, C., eds., Ninth Keck Research Symposium in Geology, abstracts volume, p. 172-175.

Mertzman, S.A., 2000, K-Ar results from the southern Oregon-northern California Cascade Range: Oregon Geology, v. 62, no. 4, p. 99-122.

Murray, R.M., in press, Geologic map of the Wocus quadrangle, Klamath County, Oregon: Oregon Department of Geology and Mineral Industries, scale 1:24,000.

Northwest Geophysical Associates, Inc., 2002, Gravity survey groundwater investigation Lower Klamath Lake Basin Klamath County, Oregon: Corvallis, Oregon, Northwest Geophysical Associates, Inc., prepared for Klamath Drainage District, May, 2002, 13 p. plus 11 sheets.

Oregon Water Resources Department, 1998, GRID: Groundwater resource information distribution, south-central Oregon, Klamath and Lake Counties: CD-ROM, 2 disks.

Palmer, A.R., and Geissman, J., 1999, 1999 geologic time scale: The Geological Society of America, product code CTS004.

Peterson, N.V., and McIntyre, J.R., 1970, The reconnaissance geology and mineral resources of eastern Klamath County and western Lake County, Oregon: Oregon Department of Geology and Mineral Industries Bulletin 66, 70 p.

Reichen, L.E., and Fahey, J.J., 1962, An improved method for the determination of FeO in rocks and minerals, including garnet: U.S. Geological Survey Bulletin 1144B, p. 1-5.

Rieck, H.J., Sarna-Wojcicki, A.M., Meyer, C.E., and Adam, D.P., 1992, Magnetostratigraphy and tephrochronology of an upper Pliocene to Holocene record in lake sediments at Tulelake, northern California: Geological Society of America Bulletin, v. 104, p. 409-428.

Sherrod, D.R., and Pickthorn, L.B.G., 1992, Geologic map of the west half of the Klamath Falls 1º x 2º quadrangle, south-central Oregon: U.S. Geological Survey Miscellaneous Investigation Series Map I-2182, scale 1:250,000.

Smith, J.G., Page, N.J., Johnson, M.G., Moring, B.C., and Gray, F., 1982, Preliminary geologic map of the Medford 1° x 2° quadrangle, Oregon and California: U.S. Geological Survey Open-File Report 82–955, scale 1:250,000.

Staudacher, T.H., Jessberger, E.K., Dorflinger, D., and Kiko, J., 1978, A refined ultrahigh-vacuum furnace for rare gas analysis: Journal of Physics E: Scientific Instruments, v. 11, p. 781-784,.

Steven, T.A., Mehnert, H.H., and Obradovich, J.D., 1967, Age of volcanic activity in the San Juan Mountains, Colorado: U.S. Geol. Survey Professional. Paper 575-D, p. 47-55.

U.S. Geological Survey, Reclamation Service, 1905, Klamath Project, California-Oregon: General Progress Map, no. 6092.

Wendt, I., and Carl, C., 1991, The statistical distribution of the mean squared weighted deviation: Chemical Geology, v. 86, p. 275-285.

Wiley, T.J., Sherrod, D.R., Keefer, D.K., Qamar, A., Schuster, R.L., Dewey, J.W., Mabey, M.A., Black, G.L., and Wells, R.E., 1993, Klamath Falls earthquakes, September 20, 1993—including the strongest quake ever measured in Oregon: Oregon Geology, v. 55, no. 6, p. 127-134.

Zoback, M.L, and Thompson, G.A., 1978, Basin and Range rifting in northern Nevada: clues from a mid-Miocene rift and its subsequent offsets: Geology, v. 6, p. 111-116.

APPENDICES—Provided as digital files on Data CD.

A Geophysical Studies

B Log of Thermal Power Company Geothermal Well

C XRF Analysis of Major and Minor Elements Methodology

D Isotopic Age Methodology

E Locations and measured water temperatures for wells in the areas surrounding the Klamath Hills.